The Impact Of Natural Dust On Outdoor PV Panels: The Performance Analysis and Short-Term Prediction

By

S. M. Shamsraj Islam
17371001

A project report submitted to the Department of Electrical and Electronic Engineering in partial fulfillment of the requirements for the degree of
Master of Engineering in Electrical and Electronic Engineering

Department of Electrical and Electronic Engineering
Brac University
September 2024

Declaration

It is hereby declared that

1. The project submitted is my own original work while completing degree at BRAC University.
2. The project does not contain material previously published or written by a third party, except where this is appropriately cited through full and accurate referencing.
3. The project does not contain material which has been accepted, or submitted, for any other degree or diploma at a university or other institution.
4. I have acknowledged all main sources of help.

Student's Full Name & Signature:

S. M. Shamsraj Islam
17371001

Approval

The thesis/project titled “The Impact Of Natural Dust On Outdoor PV Panels: The Performance Analysis and Short Term Prediction” submitted by

1. S.M Shamsraj Islam (17371001)

(Summer, 2024) has been accepted as satisfactory in partial fulfillment of the requirement for the degree of Master of Engineering on October 1st ,2024.

Examining Committee:

Supervisor:
(Member)

____

Dr. Md. Mosaddequr Rahman, PhD
Professor, Department of Electrical and Electronic Engineering
BRAC University

Internal Expert Examiner:
(Member)

____

Abu Hamed M. Abdur Rahim, PhD
Professor, Department of Electrical and Electronic Engineering
BRAC University

Internal Expert Examiner:
(Member)

____

Mohammed Belal Hossain Bhuian, PhD
Associate Professor, Department of Electrical and electronic Engineering
BRAC University

Departmental Head:
(Chair)

____

Dr. Md. Mosaddequr Rahman, PhD
Professor, Department of Electrical and Electronic Engineering
BRAC University

Ethics Statement

I have thoroughly reviewed the entire book using Turnitin and confirmed that the plagiarism level is below 30 percent. Additionally, all references in the book are properly cited.

Abstract/ Executive Summary

This study focuses on the performance of PV modules, assessing the impact of dust in a suburban area of Bangladesh. Data was collected between December 2022 and February 2023 from two photovoltaic (PV) panels, one is kept clean and other one intentionally left dusty. The analysis is divided into two sections: performance analysis and prediction analysis of PV panels. The findings reveal that, dust significantly reduce energy output, with a reduction of 5.09%, 4.75% and 3.95% in December, January and February, respectively. Additionally, weather condition (sunny and rainy) influences the short circuit current of the PV modules. The long-term effect of dust accumulation on panel performance are also evident. Furthermore, in time series analysis, the LSTM model was trained using two months of data, and its prediction for short circuit current closely aligned with the experimental data, achieving low RMSE value of 6.28 and 11.46, respectively.

Keywords: dust, solar photovoltaic, LSTM, FB Prophet. Short circuit current, Energy

Dedication

We dedicated to almighty Allah. Thank you for the guidance, strength, power of the mind, protection, skills & healthy life. All of those we offer to our Almighty. This work is dedicated to my parents for their endless love, support and encouragement.

Acknowledgement

I would like to express my deepest gratitude to my supervisor, Prof. Dr. Md. Mosaddequr Rahman, for his invaluable guidance, support, and encouragement throughout the course of this research. His insights and expertise were instrumental in shaping this thesis.

I am also grateful to my committee members, for their constructive feedback and suggestions, which greatly improved the quality of this work.

Special thanks to the members of energy research group for their constant support and for making this journey enjoyable. Your camaraderie and encouragement were essential in keeping me motivated.

Lastly, I am deeply indebted to my family for their unwavering support and patience.

.

Table of Contents

List of Tables

List of Figures

List of Acronyms

LSTM	long Short-Term Memory
RNN	Recurrent Neural Network
RMSE	Root Mean Square Error
DQ	Data In/Out
RTC	Real time Clock
SCK	Serial Clock
CS	Chip Select
IDE	Integrated Development Environment
STC	Standard Test Condition

Chapter 1

Introduction

1.1 Background

Traditional energy sources like oil, coal, and natural gas have played a significant role in driving economic growth. However, as these conventional resources are being depleted rapidly and energy demand continues to rise, global primary energy consumption saw an increase of 1.8% in 2012. [1]. With growing concerns about environmental protection, there is a strong focus on developing and advancing both clean fuel technologies and alternative energy sources. Notably, fossil fuel and renewable energy prices, along with their social and environmental costs, are trending in opposite directions, prompting changes in economic and policy frameworks to support the expansion of renewable energy markets. It is evident that the future growth of the energy sector will be largely driven by renewable energy. Transitioning to renewables can help achieve dual objectives: reducing greenhouse gas emissions to mitigate future extreme climate impacts and ensuring energy is delivered reliably, affordably, and on time. Investing in renewable energy also offers substantial benefits for energy security [1]. The sun provides enough energy to meet the world's entire energy demand, unlike non-renewable sources that are expected to be exhausted in the near future. However, a key challenge remains in efficiently converting this solar energy into electricity. When solar energy is consistently harnessed, greenhouse gas emissions released into the atmosphere are minimal. As a CO_2-free power source, solar energy has a significantly lower environmental impact compared to other power generation methods. Today, photovoltaic (PV) modules are one of the fastest-growing renewable energy technologies, known for their low carbon emissions and ease of maintenance.

Almost 99% of Bangladeshis have access to electricity as of January 2021, and the country's per capita energy output is estimated to be approximately 560 kWh as of June 2021. This is due to the use of sustainable power sources, which are intended to meet the country's growing energy needs. As of May 2021, Bangladesh's grid-tied solar system generates 129 MW of solar electricity. Up till October 2019, the public and private sectors completed and operated around 62 rooftop solar projects that are off-network and have a combined generation capacity of 14.3

MW and 50 on-grid projects with a generation capacity of 26.45 MW. RMG is Bangladesh's top export industry, with sales projected to exceed $50 billion by 2021.This industry is mostly dependent on petroleum. Of all the industries in Bangladesh, ozone depleting substance emissions account for about 38% of greenhouse gas emissions and are the largest [2]. The Ministry of Power, Energy, and Mineral Resources suggests that rooftop solar PV can be a considerate substitute to reduce the use of petroleum derivatives to some extent. In order to address the country's growing energy needs, the government recently launched the "500 MW Solar Power Mission" to support the Power System Master Plan (PSMP). Now Bangladesh can generate 635 MW (17.3%) of its annual energy from solar rooftops, and this will reduce 576,200 tons of CO_2 emissions [1].

1.2 Literature Review

Solar energy is the most dependable method to meet the world's growing energy demand as we move towards a sustainable energy source. Solar energy has the lowest carbon emissions and is the most readily available energy source. Due to the growing need for energy and the dependability of solar energy, many researchers are working harder and exploring a variety of tasks on a theoretical and practical level. On the other hand, numerous books and research papers have been published in several prominent publications and conferences. There are very few books available for comprehending the fundamental idea of how solar modules operate and how they interact with ecological aspects. Research papers and books related to the fascinating topic also offer details on previous studies and findings. The goal of the research topic has been accomplished through extensive theoretical analysis and hands-on research.

Several recent studies found the dust impact of PV modules related to Bangladesh. According to Hossain et al.[3] analyze the performance of photovoltaic solar panels due to the dust distribution on the surface of solar panels in the winter season in Dhaka, Bangladesh. Miscellaneous parameters of two pairs of panels (clean and dusty) were collected from November 2019 to March 2020. The efficiency reductions for monocrystalline and polycrystalline panels were 27.17% and 20%, respectively, on March 6, 2020 [3]. Kabir et al. show a case study analysis of dust impact on the performance of PV modules with two small PV systems at Savar, Dhaka. The first PV system was cleaned three times a day, whereas the second one was cleaned after three days. An overall 3% reduction in output power and module efficiency is found for the system, which is cleaned after three days [4].

Rahman et al. show an experimental investigation of 8-year-old 30W and 10-year-old 40W PV modules, considering dust, discoloration, delamination, and cracks. Experimental results show that the PV output power degradation rate gradually increases with dust density [5]. Alam et al. investigate the performance degradation of 10-watt old photovoltaic (PV) panels after four years in exposed outdoor conditions in Bangladesh. The maximum and minimum percentage degradation rates for four years were 5.51% and 0.89%, respectively, and the maximum annual degradation rate of each panel was 1.3775% among ten panels, and the average annual degradation rate was 0.6925% with the comparison between the measured data and the rated specifications [6]. Ahmed et al. show that PV power production is significantly impacted by dust deposition on the surface of the panel. When 42 g of dust with a 0.29 mm particle size is applied, the output power decreases by around 55.14% [7].

The impact of dust characteristics on the PV module's power output is covered by the author in the paper [8]. The amount of dust deposition on the PV module's surface causes a quantifiable drop in output power.

1.3 Objective

The goal of this study is to analyze the short-term electrical performance of the photovoltaic (PV) module, taking into account the impact of dust in a high-rise building in Dhaka city. Additionally, a short-term prediction of the photovoltaic (PV) module's short circuit has been conducted. The real-time data of each sensor has been collected from a140 foot high building between December 2022 to February 2023. The Recurrent Neural Network (RNN) models including FB Prophet and LSTM, were trained using the extracted data from each sensor and tested the predict the short circuit current output, based only on the input weather parameters.

1.4 Thesis Organization

The structure of the book is as follows: **Chapter 1** provides a general introduction, which is followed by the work's goals and foundation. The theoretical foundation of the topics discussed is presented in **Chapter 2**. **Chapter 3** outlines both the hardware setup configuration and the software used for collecting the experimental data. **Chapter 4** present the result analysis of the result, including the electrical performance of the PV module and the short-term prediction of short circuit current using three months of data for both clean and dusty solar panels. Finally, Chapters **5** concludes the study and provides recommendations for further research.

Chapter 2

Theoretical Overview

Energy extraction is shifting from fossil fuel to renewable resources worldwide. Among this, solar energy is stand out as one of the most easily and efficiently harnessed renewable resources. Considering this, the focus of this chapter is the theoretical overview of solar panels and how different weather parameters, especially dust, affect their energy output performance.

2.1 Theory of Solar Photovoltaic

The sun serves as a primary source of both solar photovoltaic and renewable energy. A photovoltaic cell, which is a type of semiconductor device, directly converts sunlight into electricity. Any device that performs this conversion is known as a photovoltaic (PV) device.

The term 'photovoltaic effect' typically refers to the generation of a voltage at the junction between two distinct materials in response to visible or other forms of electromagnetic radiation. Therefore, the study of converting solar energy into electrical energy is broadly known as photovoltaic.

Solar energy can only come from the sun. PV panels, or photovoltaic panels, are another name for solar panels. Solar panels use light from the sun to create electricity, which powers electrical appliances. A set of solar cells assembled into a unit for installation is known as a PV module. Photovoltaic cells produce direct current (DC) electricity by harnessing sunlight as an energy source. A PV panel consists of multiple PV modules, and an array is a configuration of multiple panels. Photovoltaic arrays deliver solar power to electrical devices. [9].

Solar panels come in three different varieties: i) Monocrystalline ii) Thin-film and iii) Polycrystalline. Every form of panel has advantages and disadvantages, but for this study, the polycrystalline variety has been chosen.

Table 2.1: This Table contains the Advantages and Disadvantages of the three different varieties of solar panel.

Solar panel	Advantage	Disadvantage
1. Monocrystalline	• High efficiency • Longer lifespan	• Higher price
2. Polycrystalline	• Low price	• Lower efficiency • Slightly shorter lifespan
3. Thin film	• Portable and flexible • Low weight	• Lowest efficiency

Working Principle

When sunlight reaches a solar panel, photons from the sunlight enter the solar cell, where they capture energy and release electrons from atoms. Connecting the positive and negative terminals of the cell with conductors establishes an electrical circuit, enabling the movement of electrons to generate electricity. A solar panel comprises multiple solar cells, and when many panels or modules are connected together, they form a solar array.

Semiconductor materials, such as silicon, are used to make solar cells. Insulators are materials that prevent electricity from passing through them. Semiconductor materials don't let electricity pass through them, but they can let it under specific conditions. The atoms' electrons are arranged in layers within the materials called bands or shells. Electricity can be produced by transferring electrons from the valance band to the conduction band.

It is exceedingly difficult to overcome the substantial band-gap energy of an insulator so that electricity does not flow through them since their band-gap energy is much larger than that of semiconductor materials. But if there is enough energy present in semiconductor materials, this bandgap can shatter, and valence electrons can be liberated by heating or shining on them. They will then become free electrons and be able to go up to the conduction band if their energy exceeds the energy bandgap. The energy band gap for semiconductors like silicon is 1.11 eV [9].

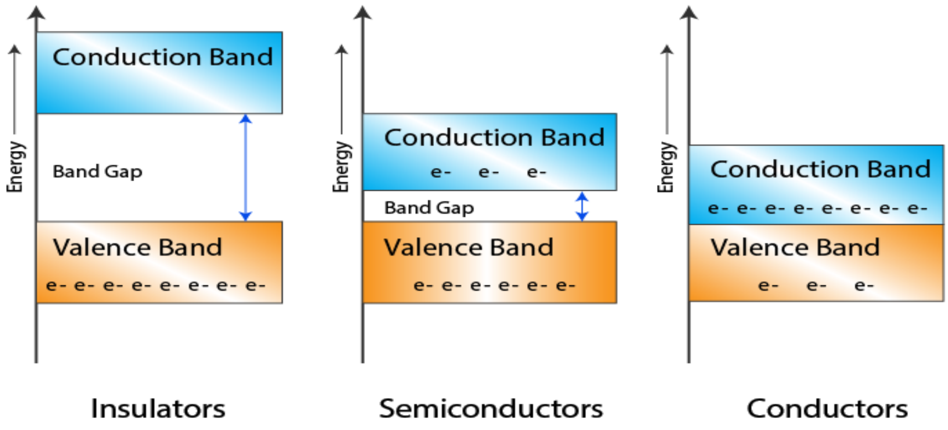

Figure 2.1: Insulators, Semiconductors, and Conductors materials

Two different forms of silicon that have been doped to allow energy to pass through them in a certain way make up a solar cell [1]. The n-type layer, or negative type silicon, is located above the p-type layer, or positive type silicon as shown in Fig. 2.1. In a sense, n-type is doped in opposition to p-type, which has more electrons, while p-type is doped because it has fewer electrons. A barrier will form at the intersection of the two materials when a layer of n-type silicon is layered on top of a layer of p-type silicon, forming a P-N junction.

Since the electrons are unable to overcome the barrier, there will be no current flow at the P-N junction. However, the photons activated the silicon atoms once they were exposed to light. The p-type (lower layer) electrons are pushed by this energy to leap over the barrier to the n-type (upper layer) and circulate throughout the circuit. Greater electrons will jump up and flow greater current when exposed to light.

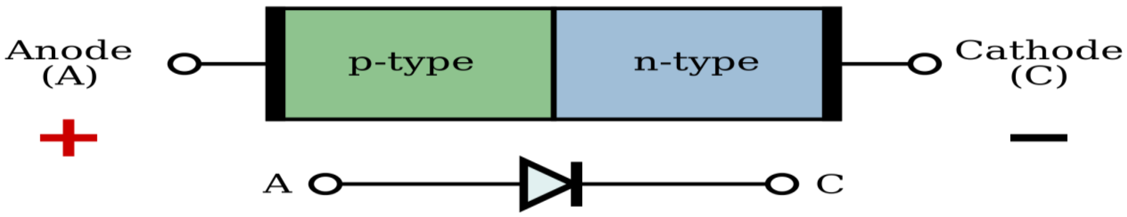

Figure 2.2: P-N Junction

Understanding the P-N junction makes it simple to comprehend how a solar panel works. The topic of discussion earlier covered the operation of P-N junctions and semiconductor materials used in solar cells, such as silicon. Solar cells make up the solar panel. This P-N junction-only cell absorbs photons when it is exposed to sunshine. By means of the photoelectric effect, electrons that take in photons will traverse the band-gap energy and go from the valence band to the conduction band, so creating electrical current throughout the circuit. Therefore, more sunlight will cause more electrons to move from the valence to the conduction band, increasing current flow. In the end, the voltage is determined by the inherent field between the P and N sides, whereas the current is dependent on the area and illumination. Figure 2.2 depicts the solar cell mechanism [9].

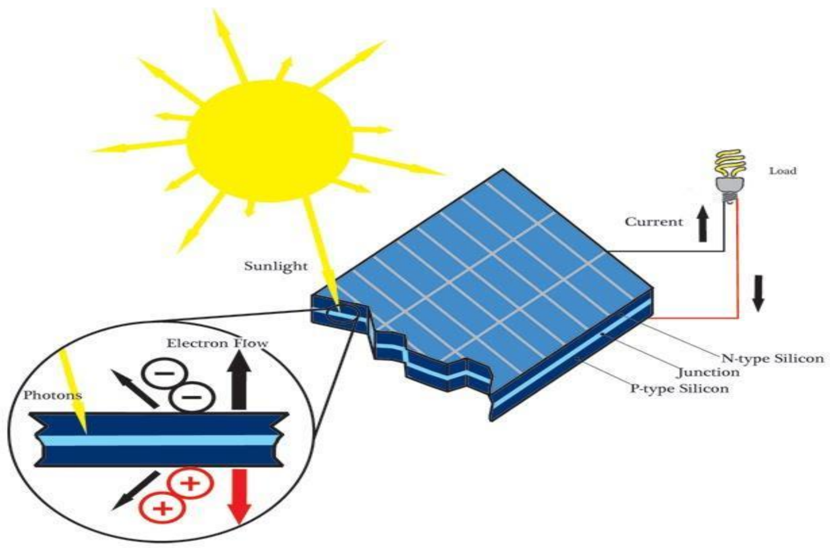

Figure 2.3: Solar Cell working Mechanism.

Single diode model

Equivalent circuit models can be used to represent the I-V characteristic curve of a cell, module, or array as a continuous function, given a certain set of operating conditions. The Single Diode model is a commonly used simple equivalent circuit type. Below is a schematic representation of a realistic solar cell's equivalent circuit:

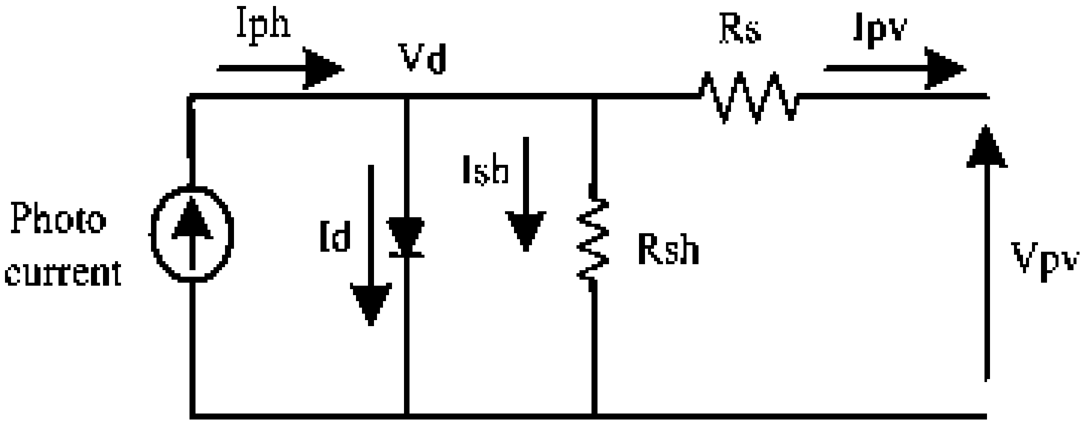

Figure 2.4: Single Diode Model

In the Fig. 2.4, a continuous current source I_{ph} is depicted, which symbolizes the light-induced current produced in the cell. This current is shown to be parallel to the P-N junction diode. The variable R_s denotes the resistance in series, whereas R_{sh} indicates the resistance in parallel (shunt) of the cell. The PV module's output current I_{pv} may be mathematically represented as [9]

$$I_{pv} = I_{ph} - I_D - I_{sh}$$

$$= I_{ph} - I_s\left(e^{\frac{q\left(\frac{V}{N_s}+IR_s\right)}{nkT}} - 1\right) - \frac{\frac{V}{N_s}+IR_s}{R_{sh}} \quad (2.1)$$

Series resistance Rs can substantially degrade solar cell performance, with Rs=0 representing the ideal case for a solar cell. It is evident that higher series resistance decreases the maximum available output power, thereby reducing cell efficiency. When Rs is large, it limits the short-circuit current. Likewise, low shunt resistance (often due to material defects) also leads to a decrease in efficiency [9].

Here,

I_S= The dark saturation current

n = The ideality factor

k = The Boltzmann's constant

q =Electronic charge

V =Applied voltage

T =Temperature

I_{ph}= Light generated current

IV Characteristics:

The IV characteristics curve of a solar cell is a combination of the IV curves of the solar cell diode under light exposure. However, the equation also includes a component known as dark current, which represents leakage current in the absence of light. [6].

The equation is given below [6].

$$I = I_0 \left[e^{\left(\frac{qV}{nkT}\right)} - 1 \right] - I_L \qquad (2.2)$$

Here,

I_0= The dark saturation current

n = The ideality factor

k = The Boltzmann's constant

q =Electronic charge

V =Applied voltage

T =Temperature

I_L= Light generated current

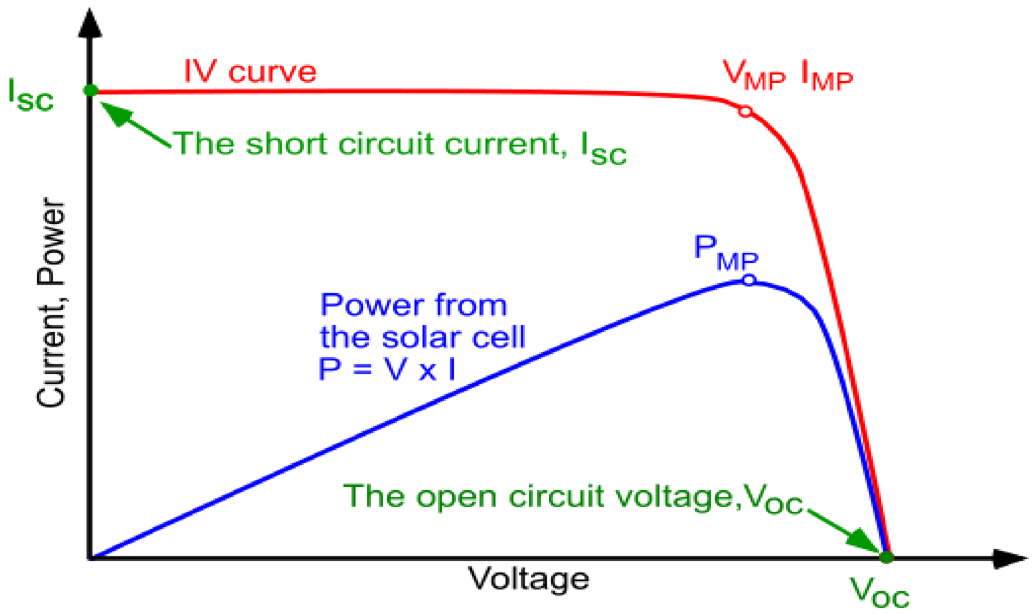

Figure 2.5: IV Characteristics curve of the Solar panel

From the IV characteristics shown in Fig. 2.4 of the solar panel several parameters can be determined such as short circuit current (I_{SC}), open circuit voltage (V_{OC}), the fill factor (FF), and the efficiency etc. The rating of the solar cell depends on these cell properties.

Short circuit current:

Short-circuit current, denoted as I_{SC} is the current generated when the voltage across the solar cell is zero. This occurs due to the creation and collection of light-induced carriers. At this point, the solar cell is effectively short-circuited, and I_{SC} represents the maximum current that can be drawn from the cell.

Reverse Saturation Current:

Reverse saturation current is a measurement of the carriers that leak over the p-n junction in reverse bias. Carrier recombination in the neutral areas on either side of the connection is the cause of this leakage. A p-n junction solar cell's ideality factor (represented by n) and reverse saturation current represented by I_O serve as indicators of the cell's quality. The reverse saturation current equation is shown below [9].

$$I_0 = \frac{I_{sc}}{e^{\left(\frac{V_{oc} \times q}{n \times k \times T \times N_S}\right)}} \tag{2.3}$$

Here;

I_{sc}= The short circuit current

V_{OC}= The open circuit current

q =Charge of an electron

k =The Boltzmann's constant

T = Temperature in kelvin

n =The ideality factor

Ns =The number of cells connected in series in the panel

Ideality Factor:

The ideality factor, represented by n, is a key property of a diode's I-V characteristics. It indicates the recombination mechanisms that govern behavior within the diode. Thus, the ideality factor serves as a measure of how closely the diode adheres to the ideal diode equation. In an ideal scenario, the ideality factor n equals 1; however, in non-ideal cases, it tends to be greater than 1. The equation for the ideality factor is provided below [9].

$$n = \frac{q \times (V_{oc1} - V_{oc2})}{k \times T \times N_s \times \ln(\frac{I_{sc1}}{I_{sc2}})} \tag{2.4}$$

Here;

q =The charge of an electron

k =The Boltzmann's constant

N_s=The number of cells connected in series in the panel

V_{oc1}&V_{oc2} is the open-circuit voltage at the same temperature with different solar irradiance

I_{sc1} & I_{sc2} is the short circuit current at the same temperature with different solar irradiance

In our experiment, we measured the open-circuit voltage and short-circuit current at nearly the same temperature but under varying solar irradiance levels. We then calculated the ideality factor using the equation provided above.

Open circuit voltage:

The maximum voltage, or open-circuit voltage (V_{OC}) of a solar cell, was obtained at zero current. Therefore, it can be said that the open-circuit voltage, which happens when the net current is zero, is the highest voltage produced by a solar module.

The equation of the open-circuit voltage is given below [9].

$$V_{oc} = \frac{n \times K \times T \times N_s}{q} \ln\left(\frac{I_{sc}}{I_{02}}\right) \quad (2.5)$$

Here,

n = The ideality factor

N_s = The number of cells connected in series in the panel

T = The temperature in kelvin

q = The charge of an electron

k = The Boltzmann's constant

I_{sc}=Short circuit current

I_{02}=Reverse saturation current

It is evident from the above equation that the open-circuit voltage increases linearly with temperature. Nevertheless, the following idea is not supported since the reverse saturation current rises quickly with temperature due to variations in the intrinsic carrier concentration. As a result, changes in open circuit voltage are dependent on both sun irradiation and temperature [9].

Fill Factor:

At both the short circuit current and open circuit voltage operating points, the solar module produces the highest current and voltage at those times, but its power is zero. The fill factor is the product of the open-circuit voltage and short circuit current multiplied by the maximum power output of the solar module. The IV characteristic curve makes it simple to determine the fill factor, which is represented by the symbol FF.

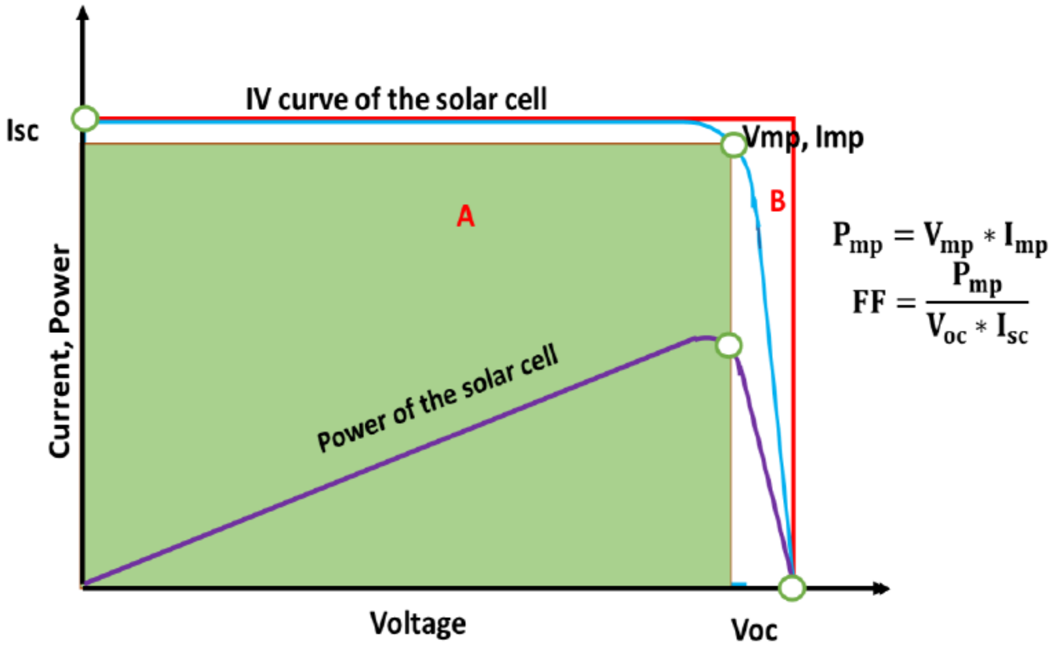

Figure 2.6: IV characteristic curve of a solar module

The maximum power can be determined by the area of the largest rectangle under the IV characteristic curve. The corners of this rectangular region correspond to the maximum voltage (V_{mp}) and maximum current (I_{mp}) that the solar module can deliver. The equation for calculating maximum power is provided below [9].

$$P_{mp} = V_{mp} \times I_{mp} \qquad (2.6)$$

The equation of the fill factor is given below [9].

$$FF = \frac{P_{mp}}{V_{oc} \times I_{sc}} \qquad (2.7)$$

In this experiment, the calculated fill factor is close to the solar module fill factor. Using this fill factor, the solar module maximum power is intended [9].

Maximum Power:

Maximum power is defined as the product of the maximum voltage and the maximum current. For the solar module used in this experiment, the maximum power is 10 W.

Experimentally the IV characteristic curve cannot be obtained daily, as the hardware setup is planted outdoor. For this reason, fill factor is used to calculate the maximum power output of the solar module. The equation of the maximum power is given below.

$$\mathrm{P_{mp}} = \mathrm{V_{oc}} \times \mathrm{I_{sc}} \times \mathrm{FF} \qquad (2.8)$$

The above formula is used to determine the maximum power for each piece of data that is collected every day from the sensors. Furthermore, there is very little, if any, difference between the calculated maximum powers derived from the fill factor and the maximum power derived from the IV characteristics curve [11].

Energy:

According to physics, energy is the quantifiable quality that is transmitted to a physical system or body and is evident in the production of work as well as in the forms of light and heat [8]. The simplest definition of energy is the capacity for work; it may take many other forms, including thermal, chemical, electrical, nuclear, and light energy. Solar panels generate power by harnessing the sun's energy. Energy from this electricity is used to power a load, such as a lightbulb. To calculate the incident cumulative light energy (Wh/m^2), the incident solar irradiance (W/m^2), is integrated with respect to Time (hour) using the trapezoidal technique of integration. (Wh/m^2), is the unit of measurement for the cumulative incident solar energy, which is computed daily.

Efficiency:

Efficiency in a power system is defined as the ratio of output power to input power. This metric is commonly used to compare the performance of different solar cells. Specifically, efficiency refers to the ratio of the energy output of a solar cell to the solar energy input it receives. Efficiency is influenced by factors such as the temperature of the solar cell, as well as the spectrum and intensity of the incident sunlight. It also serves as an indicator of the solar cell's overall performance [10].

2.2 Effect of weather parameters on the performance on PV Module

Global warming, a term used to describe increases in Earth's temperature, is a warning that we should rely more on renewable energy sources, including solar energy. Thus, sunlight is the primary energy source for extracting solar energy, and given the state of the global environment, solar energy is the most effective source. Nonetheless, several meteorological factors affect how well the solar module works. The solar module is primarily affected by the following parameters: sun irradiance, ambient temperature, module surface temperature, wind speed, humidity, air pressure, dust, height, etc. [12].

Among all these parameters, Solar-Irradiance and Temperature are the main components that affect the solar module most [10].

2.3 Effect of Dust

The performance of photovoltaic panels is significantly impacted by the characteristics of dust particles and depositions. The performance degradation caused by dust deposition or soiling has a significant impact on PV systems' viability. Numerous investigations have measured the damages brought on by dust buildup or soiling. According to the estimation, financial losses resulting from dust accumulation in 2023 are expected to range from 4% to 7% [13]. The properties of dust, including size, shape, and combination, play a crucial role in affecting light transmission to PV modules. Dust aggregation is a primary issue impacting the efficiency of photovoltaic panels. According to M. Nezamisavojbolaghi et al. [14], recent scientific studies highlight that dust accumulation can significantly reduce the efficiency and power output of photovoltaic (PV) modules. It was found that a dusty solar panel can lose nearly 50% of its power output in 30 days. Nearly 15% reduction in daily total energy due to dust, 56% overall soiling loss [14].

Knowing that, the dust layer on the panel's surface decreases the amount of radiation that penetrates into the solar cells inside the panel by absorbing or scattering the rays. When the

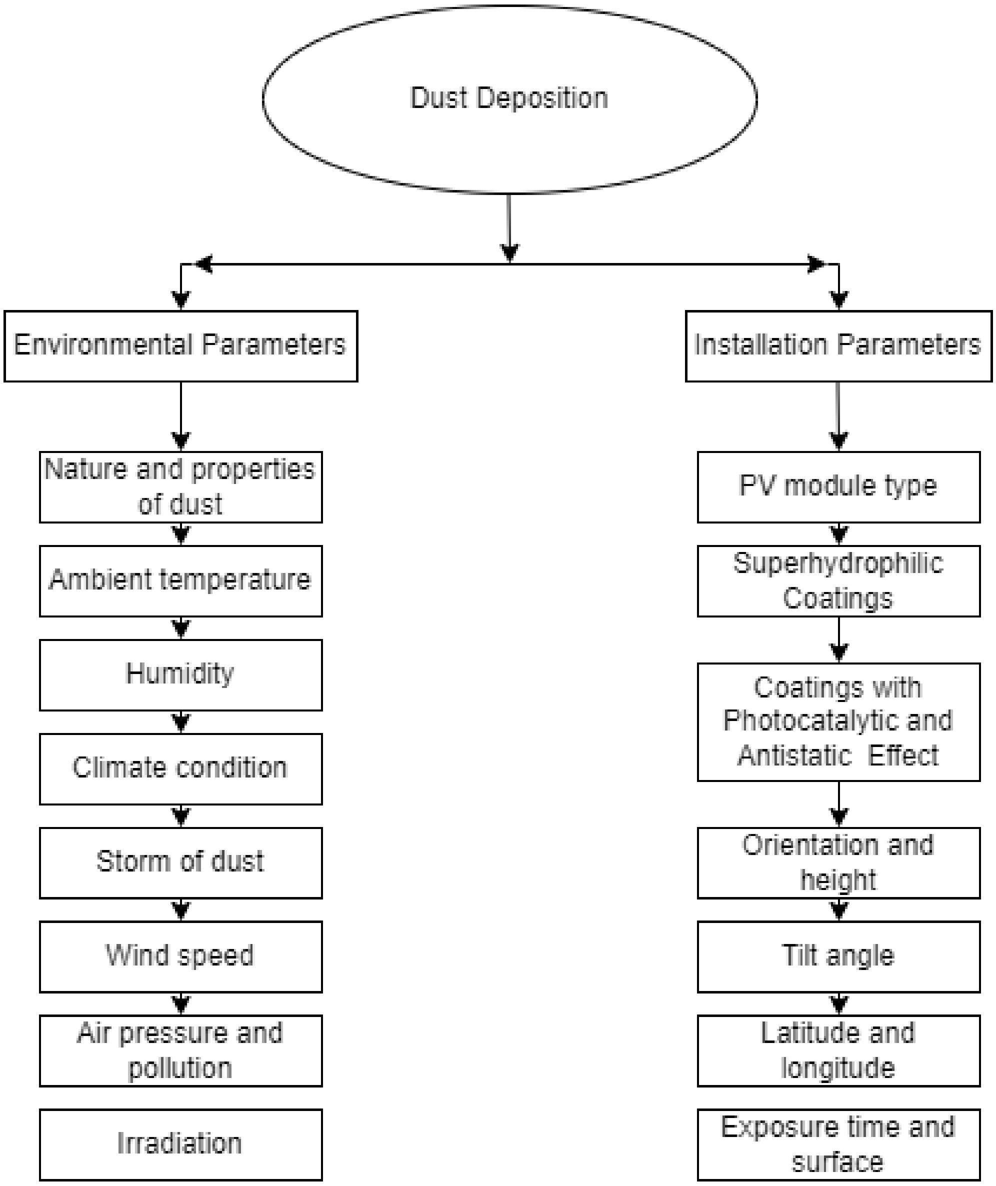

Figure. 2.7. Parameters for dust depositions [14]

values of P_{mp}, I_{sc}, I_{mp}, V_{mp}, and V_{oc} for both clean and dusty modules are examined, it can be seen that the decrease in their ratio values due to dust collection is 10.7%, 11.8%, 11.2%, 1%, and 0.5%, respectively [15]. This demonstrates that the decrease in output power is approximately equivalent to the decrease in short circuit current [15]. Figure (2.7) shows the dust deposition parameters for environmental and installation causes.

2.4 Solar Radiation

The amount of solar radiation on the surface of the planet is measured as solar irradiance (W/m^2). According to the measurement device's wavelength range, it is electromagnetic radiation from sunshine. The energy of the sun's radiation released into the surrounding environment is measured in radiant energy (J/m^2), which is obtained using mathematical operations such as integrating the solar irradiance over a certain time period. Solar irradiation, solar exposure, and solar insolation are the terms used to refer to the integrated sun irradiance [16]. The sun's height above the horizon, the meteorological conditions, and the measuring surface's tilt all affect how much solar irradiance is measured on Earth.

Solar Irradiance & Energy Calculation

The power per unit area that a solar panel receives from the sun is known as its irradiance, and it is commonly expressed in watts per square meter (W/m^2). 1000 W/m^2 is a common reference irradiance used in solar panel testing and performance assessment under Standard Test Condition STC [29]. Under perfect circumstances, such as a clear day at solar noon with the sun directly overhead, this value represents the amount of solar energy received. The short circuit current of a solar panel is the current that flows when the output terminals are shorted, indicating the maximum current the panel can generate under conventional test conditions. The correlation between irradiance and short circuit current is linear; thus, an increase in irradiance results in a proportionate rise in short circuit current [23].

The short circuit current is expressed as [29]:

$$\mathrm{I_{sc}} = \mathrm{I_{sc,ref}} * \left(\frac{\mathrm{G}}{\mathrm{G_{ref}}}\right) \qquad 2.9$$

Where:

- $\mathrm{I_{sc}}$ = Short circuit current at irradiance G
- $\mathrm{I}_{\mathrm{sc},ref}$ = Short circuit current at reference irradiance $\mathrm{G_{ref}}$
- G = Measured irradiance (W/m^2)
- $\mathrm{G_{ref}}$ = Reference irradiance (1000 W/m^2)

From this equation, we can see that, when G=1000 W/m²,

$$I_{sc} = I_{sc,ref}$$

Which means that if G is 2000 W/m² then the short circuit current will be two times than the previous value. That's why we can say that short circuit current is proportional to irradiance. As the irradiance will double, the short circuit current will also double, assuming the solar panel operates linearly.

A standardized method of assessing a solar panel's performance is to measure its irradiance at 1000 W/m² [29]. The linear relationship between short circuit current and irradiance demonstrates how the quantity of solar energy received affects solar panel output. In order to ensure that solar energy systems function properly in real-world situations, this knowledge is crucial for their design, installation, and maintenance.

The following equation was used to calculate the cumulative energy in this study. This succinctly captures the relationship between irradiance, time and energy in the context of solar energy. It provides a straightforward method to calculate the total energy received from solar radiation over a specific period [24]. The energy equation as express as:

$$Incident\ Energy,\ E = \int_{Sunrise}^{Sunset} I * dt \qquad 2.10$$

where,

- E = Energy
- I = Irradiance in W/m²,
- dt = time

2.5 Prediction Models

Time series analysis

A statistical method for examining and interpreting data points gathered or recorded at predetermined intervals of time is time series analysis. It is indexed in time order, and it records a certain metric over a period. Instead of recording data items at random or clumsily, time series analyzers do so at regular intervals over a predetermined amount of time. But gathering data over time is only one aspect of this kind of study. Each data point in a time series dataset is associated with a timestamp or time index, which indicates when the observation was made. A time series analysis of a particular data sets can provide Trend (upward or downward), Seasonality (patterns repeating itself at fixed interval), Cyclic Patterns and Noice.

When predicting the short circuit current output of a solar panel using time series models, several factors must be considered to ensure accurate forecasting. Some of these factors include the time of day (which influences sunlight intensity), seasonal variations (which affect changes in daylight hours), and the tilt of the Earth's axis. Weather conditions, such as humidity and temperature, also play a vital role. The geographic location of the solar panel installation, including latitude and longitude, influences the angle of sunlight exposure and seasonal patterns. In this paper, we have considered solar intensity and dust as the primary factors.

A time series analysis can also look at how timing impacts the dependent variable in the form of seasonality. Seasonality is characterized by patterns that repeat over specific times, such as temperature changes with the seasons. By recognizing and incorporating these seasonal patterns into our forecasts, predictions can be made that closely match real-world trends. On the other hand, macro trends are the larger-scale patterns, such as long-term changes in climate or environmental conditions. Thus, by examining both the smaller seasonal patterns and the larger macro trends, better predictions pattern about the solar panel performance can be made, aiding in more effective planning for aspects like energy usage and conservation.

Suitability of FB Prophet and LSTM Model for this study

Prediction models, FB Prophet and LSTM were selected for our study, because of the complementing advantages. LSTM offers deep learning skills for identifying complex patterns in big datasets, whereas FB Prophet offers a reliable, approachable method for seasonal and trend-based forecasting. We want to use both models to take advantage of their distinct benefits and improve the precision and dependability of our time series forecasts. A thorough analysis of the data is made possible by this dual method, which eventually results in better decision-making.

2.5.1 FB Prophet

FB Prophet is a forecasting tool created by Facebook's data science team in 2017. It's designed to predict future trends quickly and accurately in time series data. The underlying algorithm is a generalized additive model that can be broken down into three main components: trend, seasonality, and holidays. By understanding these components, FB Prophet can make reliable forecasts that capture the patterns in the data.[17]

Because it is a decomposable model, it is relatively easy to extract the coefficients of the model to understand the impact of each of these factors. The three factors can be broken down into the following equation:

$$y(t) = g(t) + s(t) + h(t) + \epsilon_t \qquad (2.11)$$

- g(t): piecewise linear or logistic growth curve for modeling non-periodic changes in time series.
- s(t): periodic changes (e.g. weekly/yearly seasonality).
- h(t): effects of holidays (user provided) with irregular schedules.
- ϵ_t: error term accounts for any unusual changes not accommodated by the model.

Prophet fits various types of functions to time, both linear and nonlinear, to understand how the data changes over time. This approach is like the one used in exponential smoothing; a technique called Holt-Winters. Essentially, it treats forecasting as finding the best-fitting curve for the data, rather than focusing on how each observation in the data relates to time specifically.

Trend is modeled by fitting a piecewise linear curve over the trend or the non-periodic part of the time series. This method also ensures that it is least affected by spikes/missing data.

To fit and forecast the effects of seasonality, prophet relies on Fourier series to provide a flexible model. Seasonal effects s(t) are approximated by the following function:

$$s(t) = \sum_{n=1}^{N} (a_n * \cos\left(\frac{2\pi nt}{P}\right) + b_n * \sin\left(\frac{2\pi nt}{P}\right)) \qquad (2.12)$$

P is the period (365.25 for yearly data and 7 for weekly data)

Parameters [$\boldsymbol{a_1}$, $\boldsymbol{b_1}$, ….,$\boldsymbol{a_n}$, $\boldsymbol{b_n}$] need to be estimated for a given N to model seasonality.

The Fourier order N is a crucial parameter that determines whether high-frequency changes can be modeled. In time series analysis, if high-frequency components are merely noise and not relevant for modeling, it is advisable to set N to a lower value. Conversely, if high-frequency changes are significant, N can be increased and adjusted based on the forecast accuracy.

One important consideration regarding FB Prophet is that it excels with stationary data. Stationary data refers to time series data that exhibit consistent behavior and maintain the same statistical properties over time. This allows for clear patterns to emerge across the years, with values remaining within a similar range. Conversely, Prophet struggles with non-stationary data, as it becomes challenging to identify the true seasonality and trends when patterns are inconsistent.

2.5.2 LSTM (Long Short-Term Memory Networks)

Long Short-Term Memory (LSTM) is a specific architecture of recurrent neural networks (RNNs) tailored for processing sequence data and capturing long-term dependencies. LSTMs possess a distinctive capability to retain information over extended periods, which makes them particularly well-suited for tasks that involve sequential data, such as time series forecasting and natural language processing. [30].

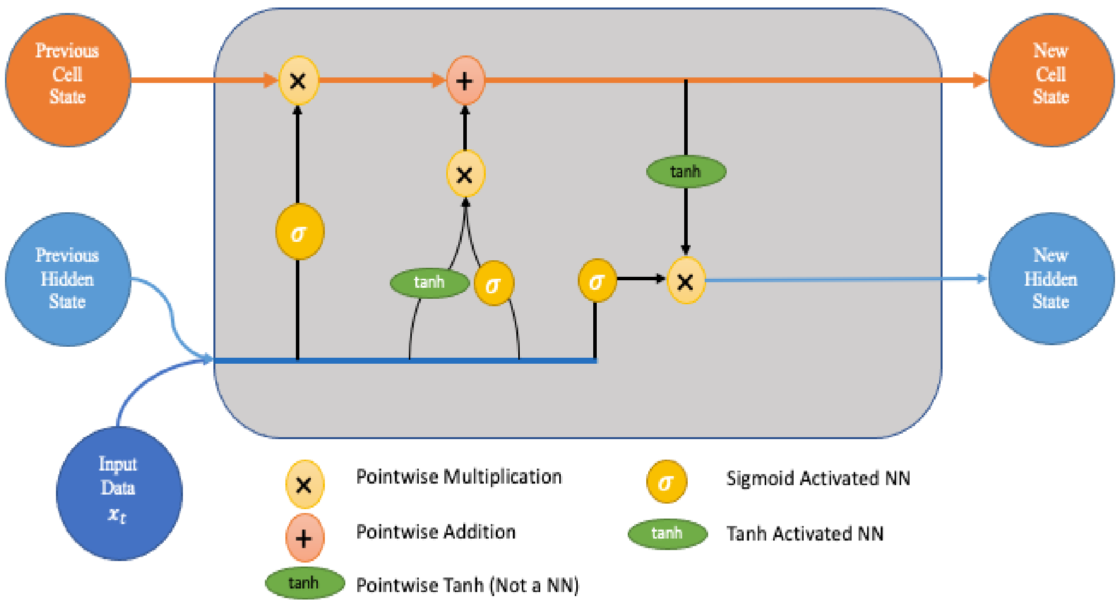

Figure 2.8: LSTM Diagram

Unlike traditional neural networks, LSTM incorporates feedback connections, allowing it to process entire sequences of data, not just individual data points. LSTM consist of memory cells that maintain a state over time and can selectively remember or forget information based on input signals. This capability allows LSTMs to capture complex temporal patterns and relationships in data. The architecture of an LSTM includes three main components: the input gate, the forget gate, and the output gate. These gates control the flow of information into and out of the memory cells, enabling the network to learn and remember relevant information while discarding irrelevant details.[18]

The chain structure of the LSTM architecture is made up of four neural networks and several memory building pieces known as cells. The gates perform memory modifications, whereas the cells store information. Three gates are present.

Forget Gate

The forget gate is responsible for removing data that is no longer necessary from the cell state. It takes two inputs: x_t (the input at the current time step) and h_{t-1} (the output from the previous cell). These inputs are multiplied by weight matrices before a bias is added. After passing through an activation function, the output is binary. If the output for a specific cell state is 0, the information is discarded; if it is 1, the information is retained for future use. The equation for the forget gate is as follows:

$$f_t = (W_f[h_{t-1}, x_t] + b_t) \qquad (2.13)$$

where:

- W_f shows the weight matrix connected to the forget gate.
- $[h_{t-1}, x_t]$ represents the concatenation of the concealed state from earlier with the current input.
- b_t is the bias with the forget gate.
- σ is the sigmoid activation function

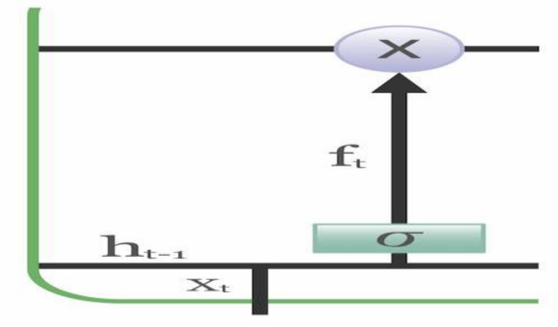

Figure 2.9: Forget gate

Input gate

The input gate modifies the cell state by adding pertinent information. Using inputs h_{t-1} and, x_t the sigmoid function is first used to regulate the information before filtering the values to be remembered in a manner akin to a forget gate.

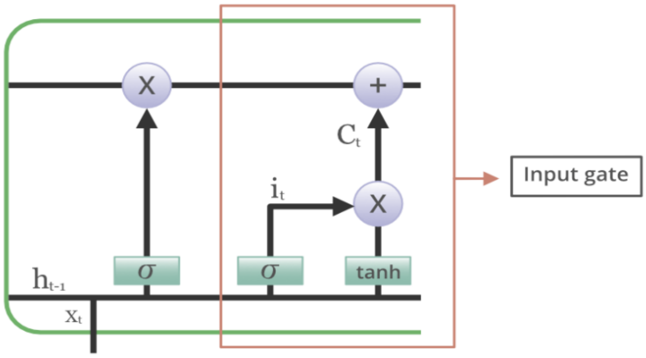

Figure 2.10: Input gate

Next, a vector containing all possible values from h_{t-1} and x_t is constructed using the tanh function, which produces an output ranging from -1 to +1.

Finally, useful information is obtained by multiplying the vector values by the regulated values [18]. The input gate's equation is:

$$i_t = (W_i[h_{t-1}, x_t] + b_i) \tag{2.14}$$

$$C_t = \tanh *(W_c[h_{t-1}, x_t] + b_c) \tag{2.15}$$

We take the information we had previously decided to ignore and multiply the previous condition by foot. We then incorporate $i_t * C_t$. This shows the revised candidate values, each of which has been adjusted for the degree to which we decided to update each state value.

$$C_t = f_t * C_{t-1} + i_t * C_t \tag{2.16}$$

Where, tanh is tanh activation function.

Output Gate

The output gate's role is to extract important information from the current cell state to generate the output. First, the tanh function is applied to the cell state to create a vector. This vector is then filtered based on the information that needs to be retained, using the inputs h_{t-1} and x_t, with the sigmoid function regulating the data. Finally, the values from the vector and the regulated values are multiplied together to serve as output and input for the subsequent cell. The equation for the output gate is as follows:

$$o_t = (W_o[h_{t-1}, x_t] + b_o) \tag{2.17}$$

Advantages and Disadvantages of LSTM

LSTM networks are capable of capturing long-term dependencies due to their memory cells, which can retain information over extended periods. Traditional RNNs often struggle with vanishing and exploding gradients when trained over long durations. LSTM networks mitigate this challenge by utilizing a gating mechanism that selectively remembers or discards information. As a result, even when there is a significant delay between important events in the sequence, the LSTM model can effectively recognize and preserve the critical context. Thus, LSTM is employed in situations where context knowledge is crucial. such as computer translation. Time series forecasting challenges like predicting stock prices, weather, and energy usage have been tackled by LSTMs. They can forecast future events by identifying patterns in time series data. Consequently, LSTMs perform better when handling time series containing many intricate patterns spread over extended periods of time. The ability of LSTMs to handle data that deviates from a straightforward pattern is another benefit. Additionally, data with various affecting elements can be processed using LSTMs. For instance, temperature, time of day, and historical energy use are all important considerations for forecasting energy use. All of these elements can be considered by

LSTMs, which can then anticipate outcomes based on the intricate relationships between them.[18]

Compared to more straightforward architectures such as feed-forward neural networks, LSTM networks incur higher processing costs. This may restrict their ability to scale in contexts with constraints or enormous datasets. Because LSTM networks are computationally complicated, training them can take longer than with simpler models. Thus, to train LSTMs to high performance, more data and longer training cycles are frequently needed [30].

2.6 Chapter Summary

The first section of the chapter, "Theoretical Background," covered the principles of solar modules. It began initially with a brief overview of the design and operation of a solar module. The explanation of how temperature affects p-n junctions is that the band-gap energy between the various energy bands determines a material's electrical conductivity. The working concept of the solar module's theoretical parameters are then explained. These theoretical parameters point to a point on the IV characteristics graph, which is known as the maximum power point, where the module has its highest voltage and current. The weather has a noticeable impact on the solar module's output power in addition to the theoretical factors influencing it. Thus, the hardware configuration employed in this experiment dynamically updates the readings of meteorological parameters with regard to time, including humidity, temperature, air pressure, and wind speed.

This chapter discusses the weather parameters and their implications. Additionally, a few fundamental angles are established to compute the incidence sun irradiance (W/m^2) on the solar module that is utilized in this experiment theoretically.

After additional integration, the cumulative light energy (W/m^2) is calculated. After that comes two different prediction models. One is FB prophet, and the other is LSTM. Both models are used to predict the future data based on weather parameters such as Temperature, Dust, Irradiance etc. How both models work have been discussed in this chapter.

Chapter 3

Experimental Setup

The primary goal of this chapter is to provide an in-depth explanation of how the hardware setup was designed and implemented. In summary, the hardware configuration was developed using various environmental variable sensors, current sensors, microcontrollers, and associated software. The sensors employed include temperature sensors, current sensors, and an RTC sensor. All these sensors were interfaced with an Arduino Uno. Data from each sensor was collected and recorded on an SD card using an SD card module, allowing for the monitoring of weather changes over time. Data has been collected from December 2022 to February 2023. The purpose of this data collection is to observe the impact of dust on the power output performance of the PV module during the dry season, as the effect of dust are more pronounced during this time compared to other seasons [3]

This chapter is primarily divided into two main sections: Hardware Implementation and Software Implementation. The Hardware Implementation section is further divided into three subsections: Data Collection System, Sensor Brief Description, and Connection Diagrams Explanation. These subsections detail how the system operates and collects sensor data, provide descriptions and performance evaluations of each sensor, and explain how the sensors are connected to the microcontrollers. The Software Implementation section is also divided into three subsections: Data Extraction System and Software Brief Description. In these subsections, the methods for data extraction and the software tools used for data gathering are discussed, along with flowcharts illustrating the interfacing of all the sensors.

3.1 Hardware Implementation

In this section, the data collection system using Arduino-UNO is explained with detailed connection diagram. Also, a brief description and performance of each sensor are shown in this section.

3.1.1 Data Collection System

The hardware configuration is partitioned into two sections in order to alleviate the burden on microcontrollers. Within a specific component of the system, an Arduino Uno is exclusively responsible for gathering data from a DS18B20 Temperature sensor and an INA219 Current Sensor. This data is then stored on an SD card with the assistance of an RTC sensor. Within a different section of the system, an additional Arduino Uno is specifically allocated to retrieving short circuit current data from a dusty solar panel using the INA219 Current Sensor. This data is then stored in a separate SD card module, facilitated by the RTC sensor. The Arduino Uno was programmed in a way that all the sensors can collect data after every 20 seconds. This applies to Temperature sensor, INA219 current sensor, and RTC sensor. After every 20 seconds microcontroller will send the data to SD card module to record the data. The data is recorded in a row starting from left to right, starting from Date, Time.

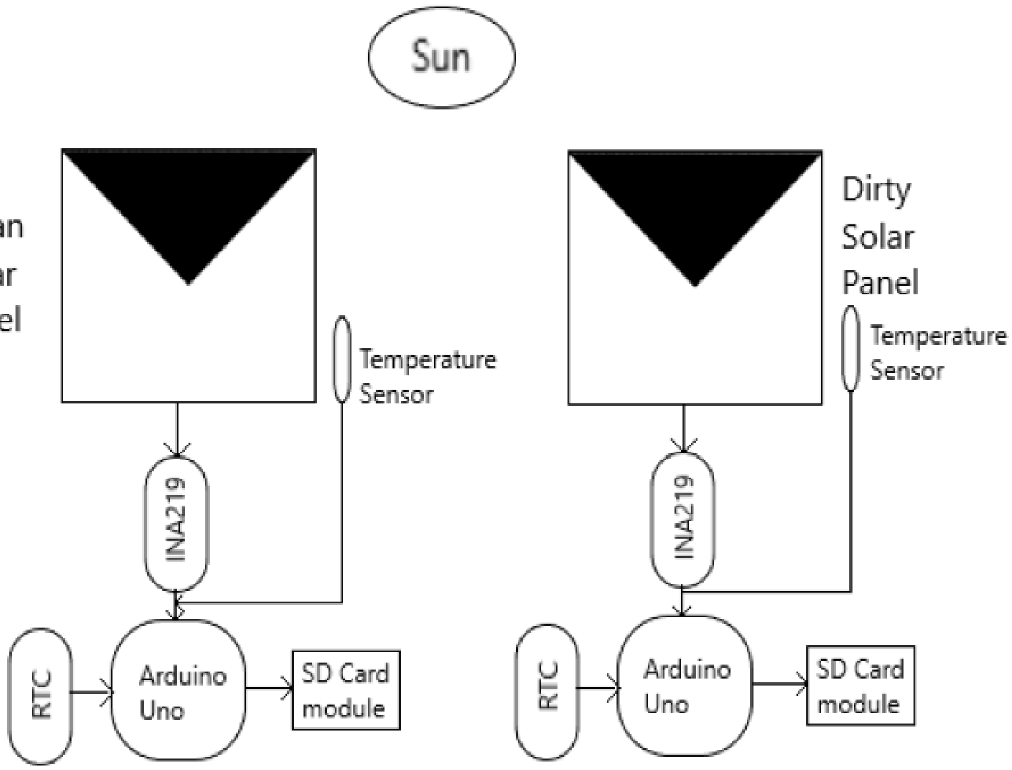

Figure 3.1: Block Diagram of Hardware setup

3.1.2 Sensor Description

INA219 Current Sensor

The INA219 is a device that measures current and monitors power on the high side of a circuit. It is equipped with an I2C interface. The INA219 is capable of monitoring both the voltage drops across a shunt resistor and the supply voltage [19]. It can adjust the conversion timings and apply filtering as needed. By utilizing a configurable calibration value in conjunction with an internal multiplier, it becomes possible to obtain direct readouts in amperes. A supplementary multiplier registers computed power in Watts. The I2C interface provides 16 programmable addresses. The INA219 detects voltage differences between shunts on buses ranging from 0V to 26V. The gadget operates on a power source ranging from +3V to +5.5V and consumes a maximum of 1 mA of electricity from the supply. The module has a maximum current measurement capability of ±3.2A with a precision of ±1%. Additionally, it has a resolution of ±0.8mA. It employs 0.1ohm 2W shunt resistor to detect current.[19]

The INA219 operates within a temperature range of -40°C to +125°C. It features six pins, with the VCC and GND pins connected to a power source of 3V to 5V to power the module. The I2C pins (SCL and SDA) are connected to the microcontroller's I2C pins, while Vin+ and Vin- are utilized for measuring the source voltage and supplied current. To measure the source voltage, a load must be connected to the source. However, since the device is designed for measuring short-circuit current, no load is used in this scenario, which prevents the device from measuring the source voltage.

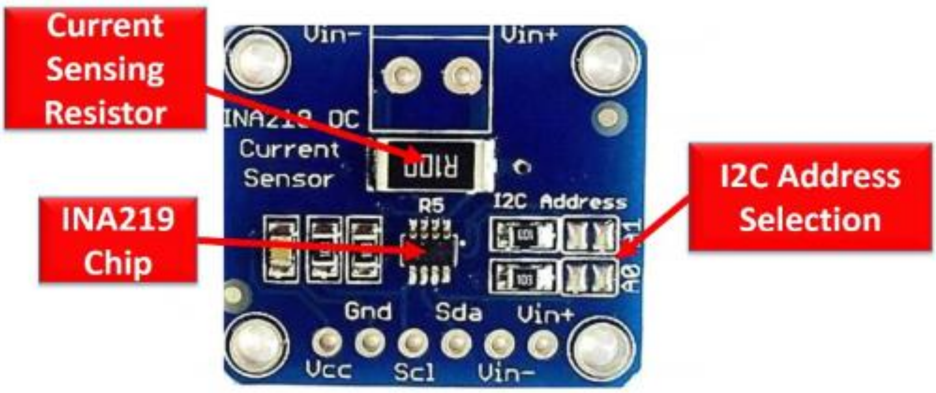

Figure 3.2: INA219 Current Sensor

DS18B20 Temperature Sensor

A programmable temperature sensor is the DS18B20. The most common use for it is temperature measurement. This version contains characteristics that make it waterproof. While measuring temperatures between -55°C and 125°C is safe for it, temperatures up to 100°C are advised. Since it offers a digital signal, there is no signal loss. In the range of -10°C to +85°C, the sensor can provide temperature data with an accuracy of ±0.5°C. 3 to 5 volts are needed for the sensor's input. In other words, the microcontroller can supply electricity. Three pins make up the sensor: DQ (Data In/Out), VDD (Power Supply Voltage), and GND (Ground). The temperature of the device is indicated via the 9–12-bit (adjustable) temperature readings provided by the DS18B20 Digital Thermometer. The DS18B20 communicates temperature information to Arduino via a 1-Wire interface, requiring only one wire—along with ground—to be connected between a central CPU and a DS18B20. You can extract power from the data line itself to read, write, and convert temperatures. It is necessary to attach a pullup resistor (4.7KΩ) between the data pin and VDD when connecting the sensor to the microcontroller.[20]

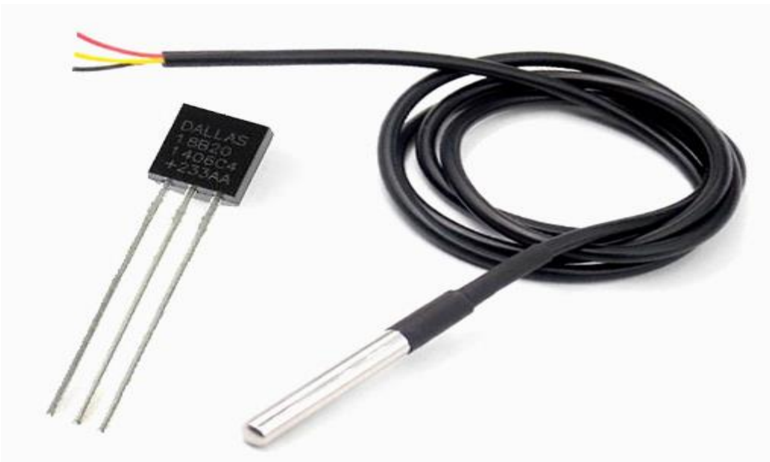

Figure 3.3: DS18B20 Temperature Sensor

DS3231 Real Time Clock

Although the Arduino board has a built-in timekeeper, the Arduino Project employed a separate RTC module. Since the Arduino clock resets when the power source is off, the device uses an external clock module.

The DS3231 module has an integrated battery, which allows the RTC module to maintain real-time tracking even if the device's power is cut off. A cheap, very accurate real-time clock that can keep track of hours, minutes, and seconds in addition to the day, month, and year information is the DS3231. Additionally, it automatically adjusts for leap years and months having fewer than thirty-one days. Four wires are required: two I2C communication ports, SDA and SCL, and the VCC and GND pins for powering the module.[21]

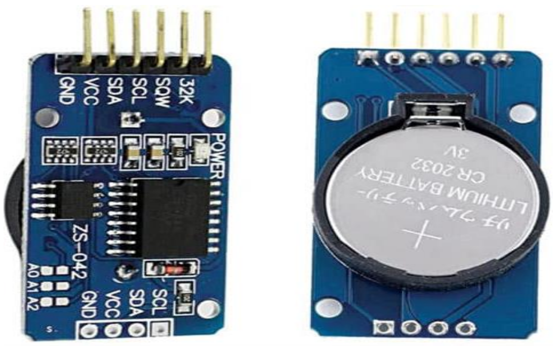

Figure 3.4: DS3231 Real Time Clock

SD Card Module

Among the storage options for devices like smartphones, minicomputers, and other gadgets, SD and micro-SD cards are among the most useful. It is possible to write or read data on memory cards and communicate with them via the SD and micro-SD card modules. The module uses 3.3V to 5V and communicates with the SPI standard. The SD library is required in order to use these modules with Arduino. By default, the Arduino program has this library installed. All of the Arduino data is automatically stored on an SD card upon installation and coding. This project involves changing the code to record temperature and short circuit data in the following order: Date, time, temperature, current, count number, and name of the day should all be saved in a (.txt) file.

Figure 3.5: SD card Module

3.2 Hardware Setup

In the hardware setup, two circuits were constructed using two Arduino Uno boards, two INA219 current sensors, and two DS18B20 temperature sensors. The implementation of two circuits was intended to reduce the load on the microcontrollers.

After setting up a solar panel, two wires are connected to INA219 Current sensor through Vin+ and Vin- pins. To connect the INA219 current sensor to the microcontroller, SCL and SDA pins of the current sensor were linked to the A5 and A4 pins that works as dedicated SCL and SDA pins. Then to power up the current sensor, V_{cc} and Gnd pins of the current sensor linked to the 5v and GND pin of the Arduino Uno. Then follows the DS18B20 Temperature Sensor, where there are V_{dd}, DQ and Gnd pins. The V_{dd} and Gnd of the Temperature sensor connected to 5v and GND of the Arduino Uno. The DQ is a one wire data bus that is attached to the Digital 6th pin of the Arduino Uno. Regarding the RTC DS321 Sensor, we need to establish connections between it and the microcontroller using 4 pins. The SCL and SDA pins are connected to pins A5 and A4, respectively, on the Arduino Uno. The V_{cc} and GND pins of the RTC sensor are linked to the 5V and GND pins of the Arduino Uno. Finally, the SD card module, which is responsible for storing data, is attached to the Microcontroller using six pins.

The V_{cc} and GND pins are linked to the 5V and GND pins of the Arduino Uno. The MISO (Master in Slave Out) signal refers to the Serial Peripheral Interface (SPI) output from the microSD card module, which is coupled to the D12 pin of the Arduino Uno. The MOSI (Master Out Slave In) is the Serial Peripheral Interface (SPI) input that is connected to the D11 pin of the Arduino Uno and is used for communication with the microSD card module. The SCK (Serial Clock) pin receives clock pulses from the master device (in this case, an Arduino) to synchronize the transfer of data.

It is attached to the D13 pin of the Arduino Uno. The chip select (CS) pin is linked to pin D4 on the Arduino Uno.[22]

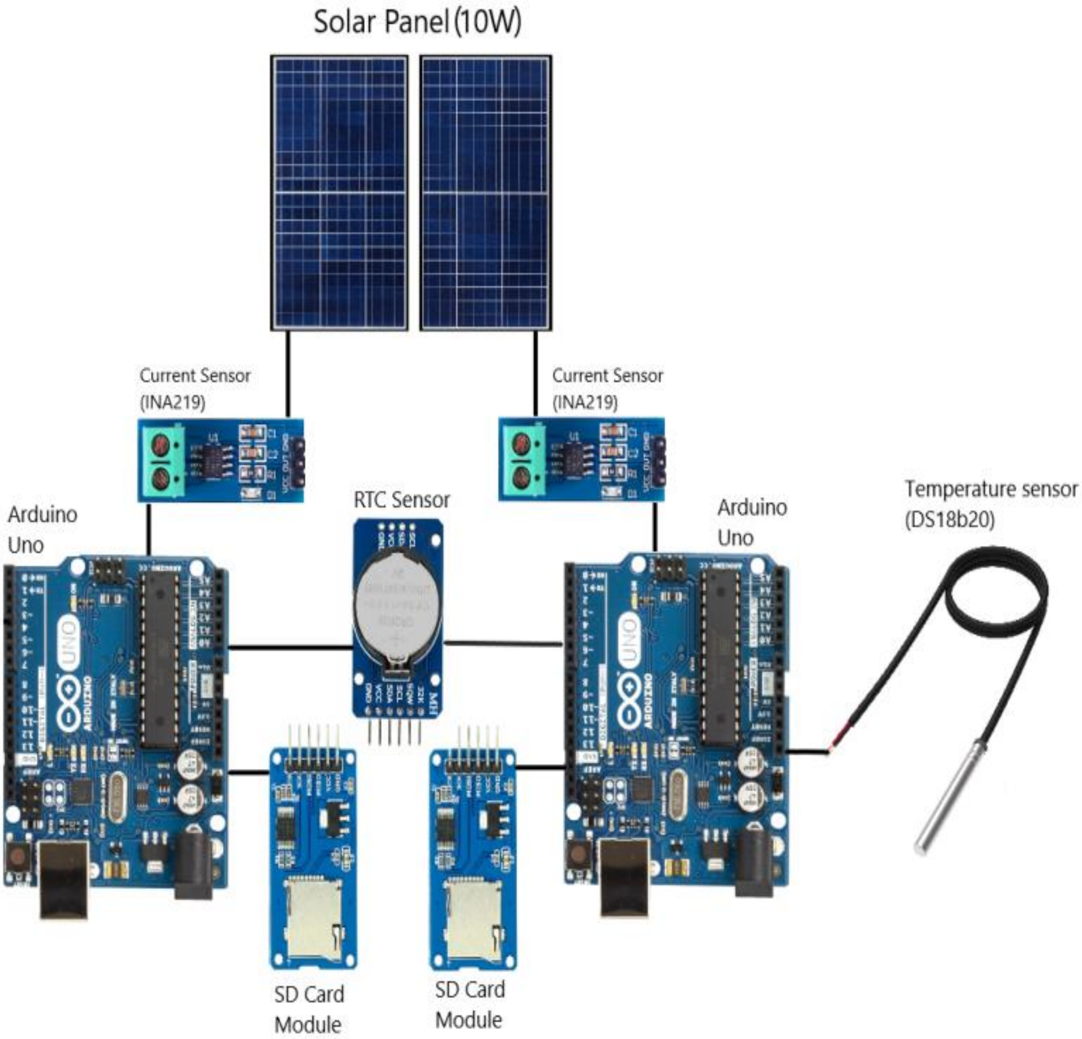

Figure 3.6: Circuit Diagram

The same circuit was built for another solar panel as well. They were set up in two different containers, so that no dust and debris can cause any malfunction of the circuits.

Figure 3.7: Experimental Setup on the top of Building 4, BRAC University.

3.3 Software Description

Programming Arduino microcontroller boards is done via a software package called the Arduino IDE (Integrated Development Environment). It offers a user-friendly interface for creating, assembling, and uploading code to boards that are compatible with Arduino. On Windows, macOS, and Linux operating systems, the IDE may be used without charge and without any limitations.

Writing code for Arduino boards is made easier by the Arduino IDE, which offers a library of examples and libraries that users may use to get started on their projects quickly. The supported programming languages include Arduino, Wiring, C++, and C, along with their acronyms. To communicate with sensors, actuators, and other electrical components attached to the Arduino board, users can write code.

The Arduino IDE provides real-time debugging and interactive development capabilities for developers working with the Arduino board. Features like automated code indentation, syntax highlighting, and serial monitoring are included in this program.

All things considered, the Arduino IDE is a vital tool for creating projects with microcontroller-based systems that professionals, students, and amateurs may use.

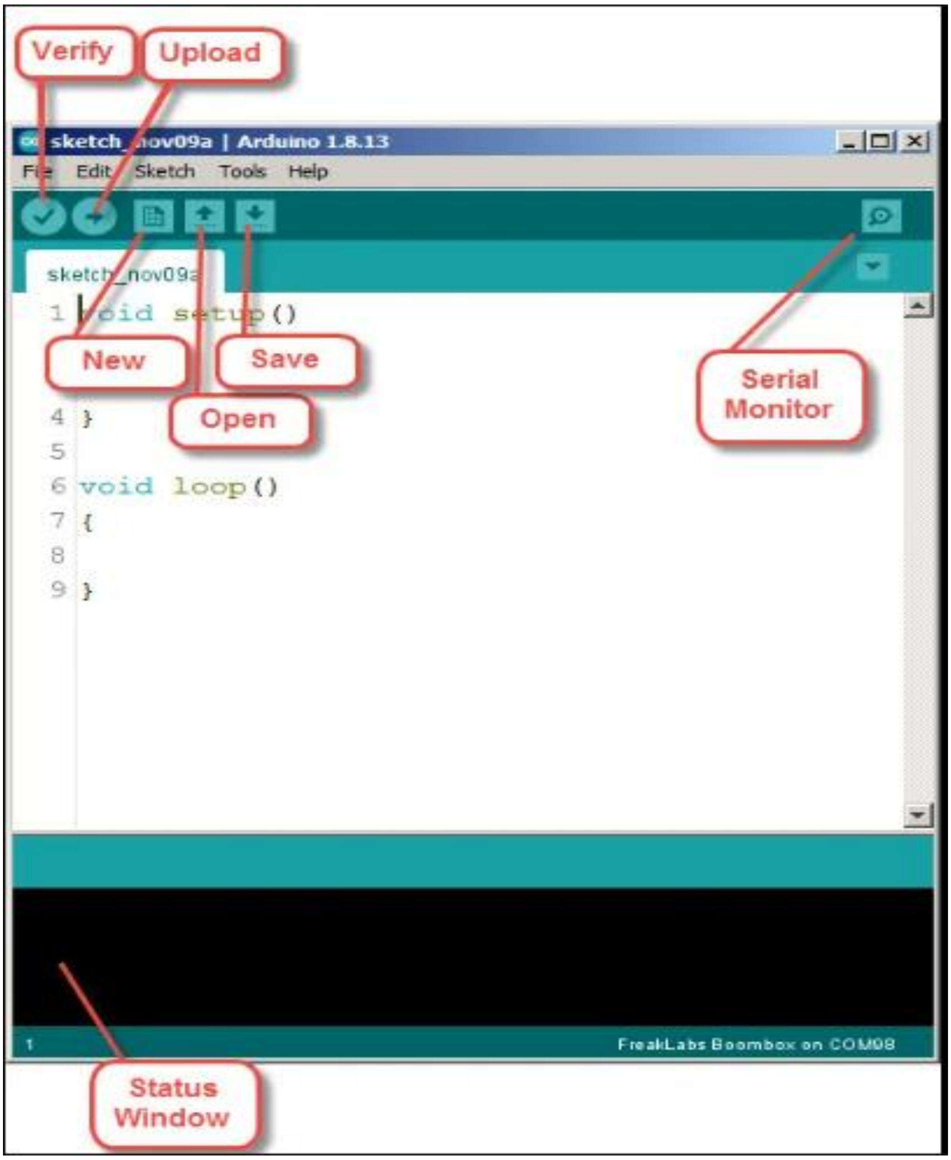

Figure 3.8: Window of Arduino IDE

Challenges Faced

This hardware configuration has been operational since December 2022. This hardware arrangement was built and maintained with many challenges. The setup was located on the roof of BRAC University Building-4. The challenges encountered are:

i. Data Loss: Since every sensor's data was required from dawn to sunset and the building's energy supply is turned on around 7.30and there was a significant amount of data loss.

ii. Power cuts: Due to intermittent access to the site, it could not be easy to check if the hardware setup was receiving power throughout the day or if there had been any blackouts or interruptions in the electrical supply.

These were the primary issues that were encountered initially. Data storing maintain proper time was resolved once the RTC sensor installed. Although blackouts occasionally cause the system to lose data.

Features:

i. Microcontrollers and sensors may be replaced if they become damaged.

ii. The system can gather dust and temperature environmental data.

iii. Proper time maintenance while data logging even after blackouts.

For over 3 months, the hardware setup has been operating and gathering experimental data. The goal is to keep it going for at least a year, and preferably longer. As the training dataset grows, the generated machine learning model becomes more accurate in its predictions. In order to improve the model's accuracy, precision, and dependability, the objective is to gather as much data as feasible.

3.4 Chapter Summary

The hardware setup and software implementation are the two primary sections of this chapter. The hardware setup's construction, the electronic equipment employed, their connections inside the system, and the way the Arduino Uno microcontroller gathered sensor data are all significant facts. In a similar vein, the software setup process explains how the data are taken from the Arduino Uno, what applications were utilized, and how each sensor's code operates.

Chapter 4

Result and Discussion

This chapter presents a theoretical analysis of the sensor data collecting process. Data collection began in December 2022 and continued for three months after the circuit was built. To facilitate understanding of the experimental data analysis, this chapter is divided into three main sections. For the performance analysis and snort term prediction of the PV module’s short circuit current, the sensor data needs to be converted from notepad format to Excel format. The raw data analysis and relevant information are covered in this first section. In addition, it examines the solar panel's performance in relation to weather conditions and the way dusty and clean modules function due to the way dust breaks down on the panel's surface. Rather, in both ideal and experimental circumstances, solar irradiance is computed or measured using theoretical information. Temperature affects solar module performance the most out of all the environmental factors. Other than that, solar irradiance has a significant impact on solar module performance. The final section discusses the parameter analysis that was done utilizing the solar panel's I-V characteristics curve. The I-V characteristic curve makes it possible to evaluate the overall behavior of the solar panel with efficiency and effectiveness using this simple approach.

4.1 Raw Data Analysis

The temperature, clean and dusty short circuit current data is collected at a rate of three times per minute, and time is a significant component in the study. Weather conditions should also be taken into account in order to better understand how well solar panels perform. When comparing two modules, one should be cleaned on a regular basis, while the other should be cleaned when it is first installed. Over time, dust particles will accumulate on the panel's surface. The performance of the solar module is affected by several factors besides temperature and dust, including cloud cover, sun irradiance, the position of the sun, the area's location, etc. PV module's short circuit current is influenced by weather conditions and, moreover, primarily by solar irradiance. Additionally, the impact of weather conditions may be easily noticed using a straightforward approach like the sensors data vs. time plot. And by comparing the performance of the dusty and clean solar panels, the effect of dust particles on the PV module can be revealed. Over the course of these three months, the weather station has continually gathered about 2260 data points every day for each sensor. The data gathering process begins at 7.30 am and finishes at 6:00 pm.

The primary focus will be on how dust particles affect the solar module short circuit current performance. Both the Clean and Dusty panels were cleaned at the time of installation; as a result, they performed similarly, indicating that their short circuit currents are the same or very near to one another. To put it another way, the clean and dusty modules' short circuit currents I_{sc} plot overlap with one another. Over time, dust particles gather on the surface of the dusty panel, leading to a considerable decline in the dusty module's performance as compared to the clean module.

Now if we look at how each solar panel performs next to each other after installing them on the rooftop. The installation was completed on December 1st. After five days we can see that there is a small difference in the output of both solar panels. As the dust accumulates on the surface of the dusty solar panel, the short circuit current output decreases in comparison to that of the clean panel which is shown in Figure. 4.1.

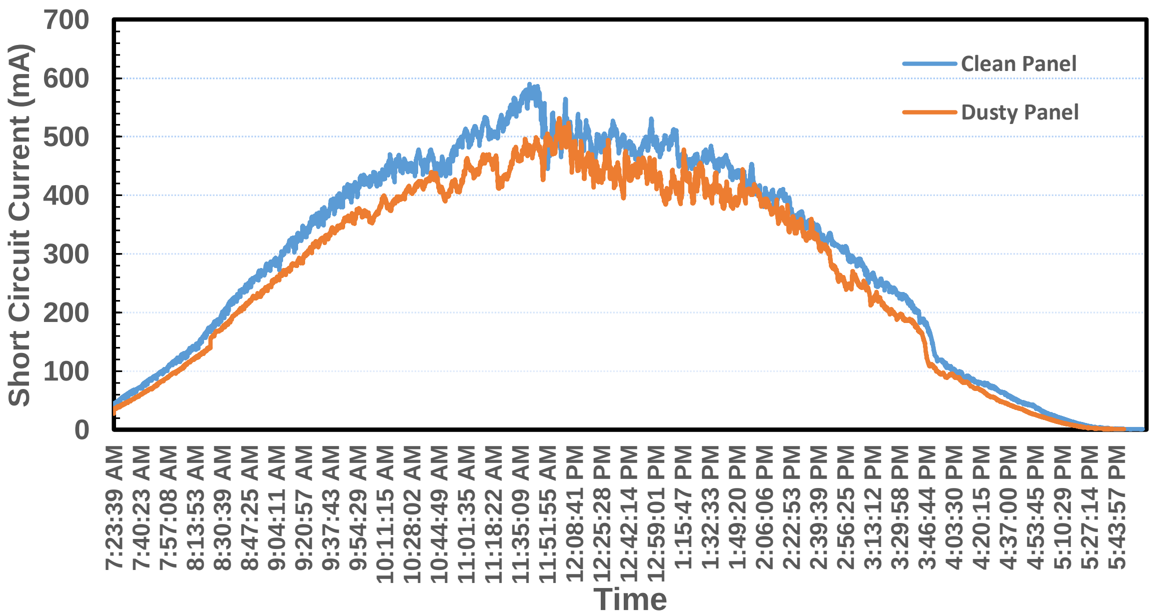

Figure 4.1: Plot of the Short Circuit Current of both clean and dusty Solar Panel collected on December 5th

Figure 4.2 shows the percentage difference of Short Circuit Current of both clean and dusty panel, collected on 5th December. Since it's only been five days, the amount of dust accumulation on the panel may still be minimal, causing times when the performance difference is close to zero. Dust can take time to build up significantly, and in the early days, small or uneven accumulations may have less noticeable effects on the panel's output.

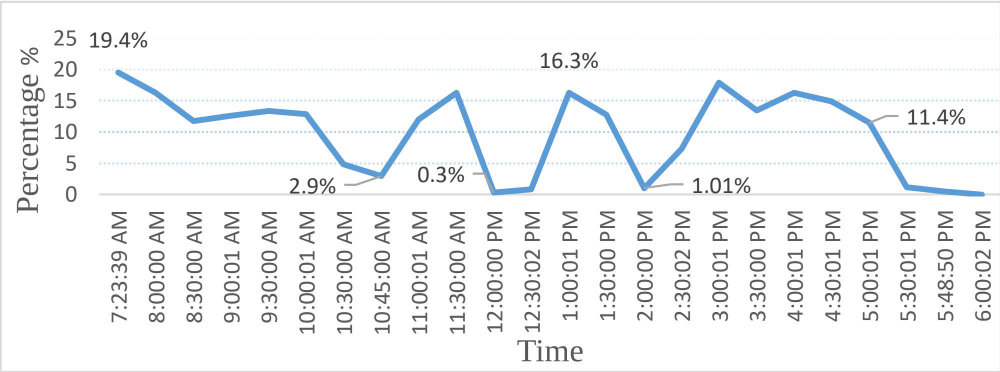

Figure 4.2: Plot of the percentage difference of Short Circuit Current between clean and dusty panel, collected on 5th December

Refereeing to the plot from December 15, it was evident that the day was overcast, as shown in Figure 4.3. It can also observe that as the intensity of the sunlight (solar irradiance) increases, more electrical current can be produced by PV module, directly increasing the short circuit current [23][24]. As solar irradiance increases, the output short circuit current from both panels rises as well, but the amounts differ slightly because of the dust buildup.

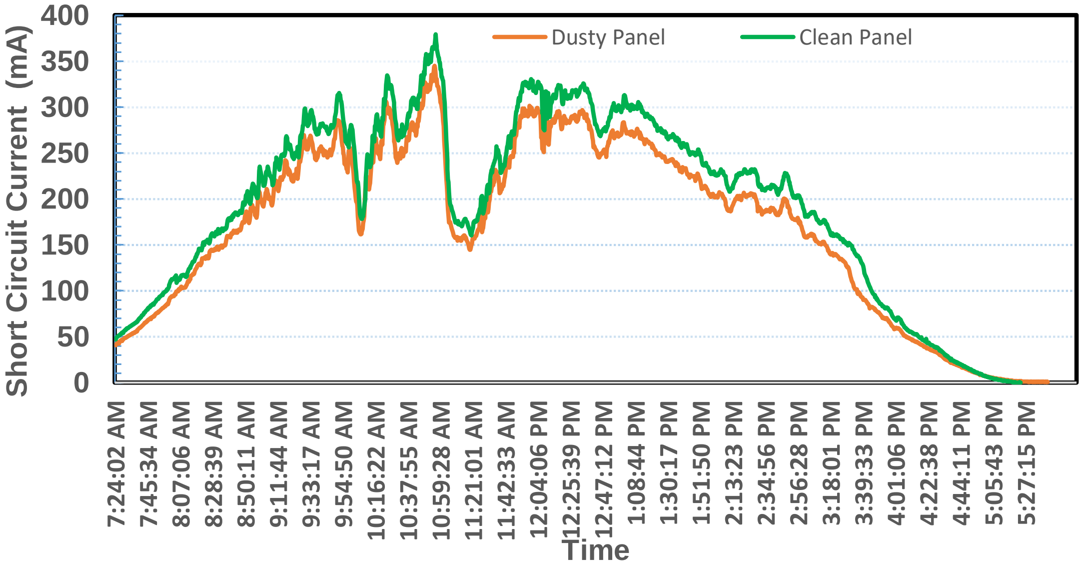

Figure 4.3: Plot of the Short Circuit Current of both clean and dusty panel, collected on 15th December (Cloudy Day)

After 10.50 AM on December 15, solar irradiance decreases, as the solar intensity drops the short circuit current output from both the panels also decline [23]. Following 11:30 AM, as solar intensity increases the short circuit current output for both panels rise accordingly. On December 15th, the highest short circuit current was 379.2mA for the clean solar panel and 344.9 for the dusty solar panel respectively.

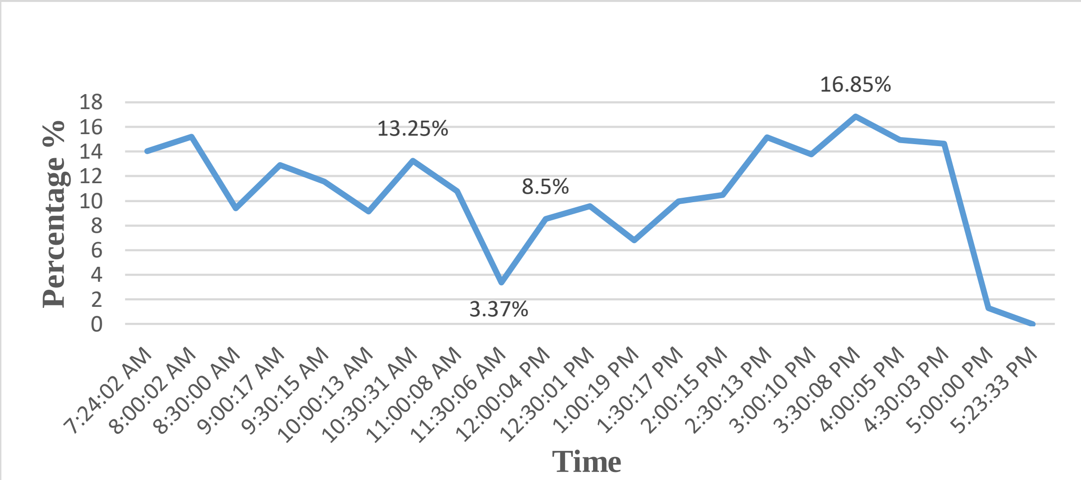

Figure 4.4: Plot of the percentage difference of Short Circuit Current between clean and dusty panel, collected on 15th December

The percentage difference plot in Figure 4.4 shows, a drop of solar irradiance leading to decrease in the percentage difference between clean and dusty panel from 13.25% to 3.37%. When solar irradiance was high, dust has a more significant impact on the output of the dusty panel compared to the clean panel. However, in low irradiance condition, the overall output drops for both panels resulting in smaller absolute difference in their performance.

Here at 10.50am the clean panel's output drops significantly due to reduce irradiance, while the dusty panel's output also drops but is still relatively lower rate, so the percentage difference decreases 13.25% to 3.37%.

Additionally, from the Figure 4.4 it is evident that, solar irradiance condition has changed after the initial drop (sky cleared and solar irradiance increased again), the clean panel benefited more from the increased in irradiance compare to the dusty panel. The clean panel reached a higher output, while dusty panel, hindered by dust, wasn't increased as significantly, thus increase percentage difference by 8.5%.

Now on 24th December we can see a clear graph Figure 4.5, where the difference between the clean solar panel and the dusty solar panel is very prominent. The peak value of the short circuit of the clean solar was 643.4 mA, where the max output current of the dusty solar panel was 503.8mA. So, there is a clear difference of 139.6mA, which is approx. 21.7% lower than the clean module, because of the dust accumulation on the solar panel.

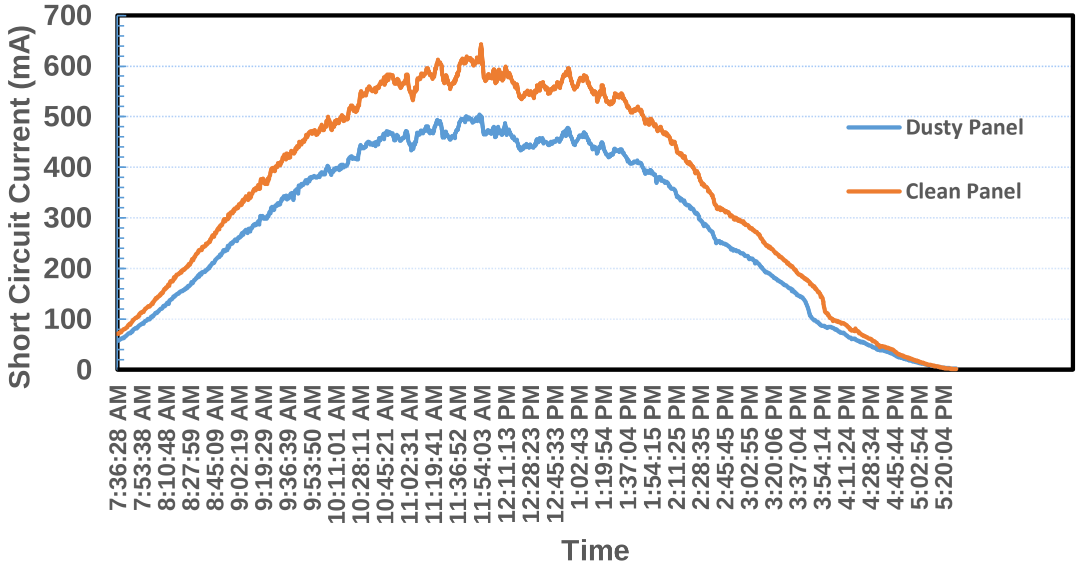

Figure 4.5: Plot of the Short Circuit Current of both clean and dusty solar panel collected on 24th December (Sunny Day)

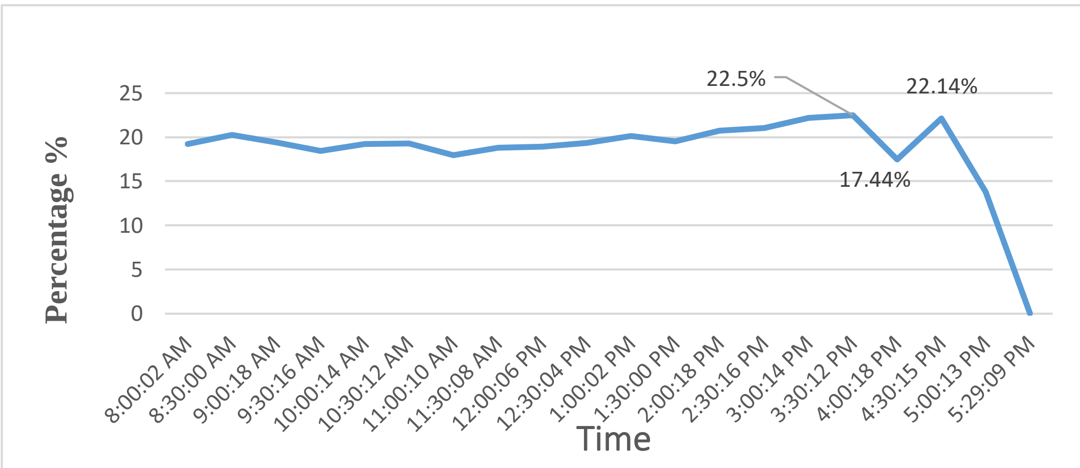

Figure 4.6: Plot of the percentage difference of Short Circuit Current between clean and dusty solar panel collected on 24th December (Sunny Day)

Similarly, the percentage difference plot in Figure 4.6 demonstrates minimal fluctuation, as the data was collected on a sunny day with a stable solar irradiance. This indicates that there was a little variation solar irradiance, resulting the percentage difference remaining nearly constant.

Now that we have the data for 9th January, we can also see from the graph Figure 4.7 that it was an overcast day. We can also observe from the figure that as solar irradiance increases, the output short circuit current from both panels rises as well [23].

However, the output differs because of the buildup dust particles. The sunlight intensity drops on January 9th after 12.30 PM. As the solar irradiance declines, both panels' output short circuit current decreases as well [23]. Following 01:00PM, both the panels' output short circuit current started increasing as the solar irradiance increase once more. On that day, the

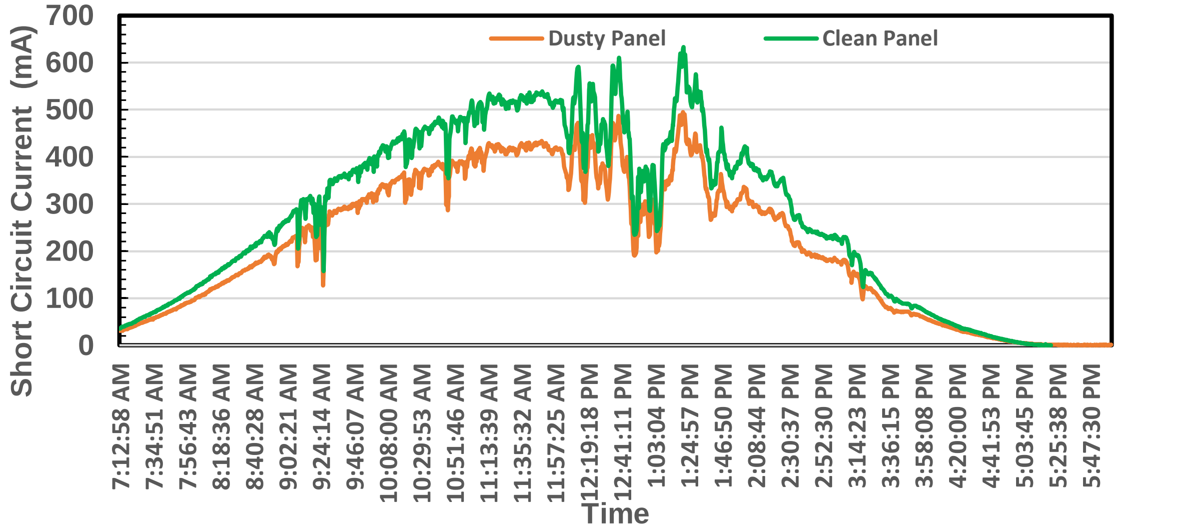

Figure 4.7: Plot of the Short Circuit Current of both clean and dusty solar panel collected on 9th January (Cloudy Day)

peak current of the clean module was less than 632 mA, Whereas the dusty solar panels max output was 495mA.

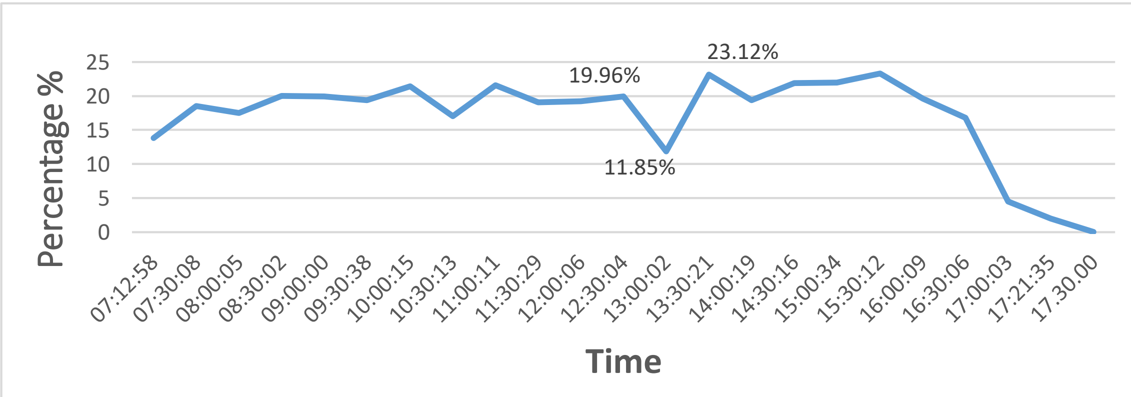

Figure 4.8: Plot of the percentage difference of Short Circuit Current between clean and dusty solar panel collected on 9th January (Cloudy Day)

Moreover, Figure 4.8 shows, after the sudden reduction of percentage difference 19.96 % to 11.85%, at 1.00pm the increase in percentage difference to 23.12% attributed that further accumulation of dust affecting the dusty panel's performance and change in solar irradiance favors the clean panel more significantly.

The same can be said for the output of 12th January. It can be seen from the Figure 4.9 that it was a sunny day, and the output short circuit current of the clean solar panel is higher than the current of the dusty solar panel. Max current of the clean solar panel was 579.2mA and the max current of the dusty solar panel was 505.6mA. The percentage difference graph for the same (Figure 4.10) day shows some fluctuation, indicating that dust has a non-linear effect on panel performance [25]. Once dust accumulation reaches certain level, the performance of the dusty panel can drop dramatically compared to clean panel [25], resulting in significant variation in percentage difference.

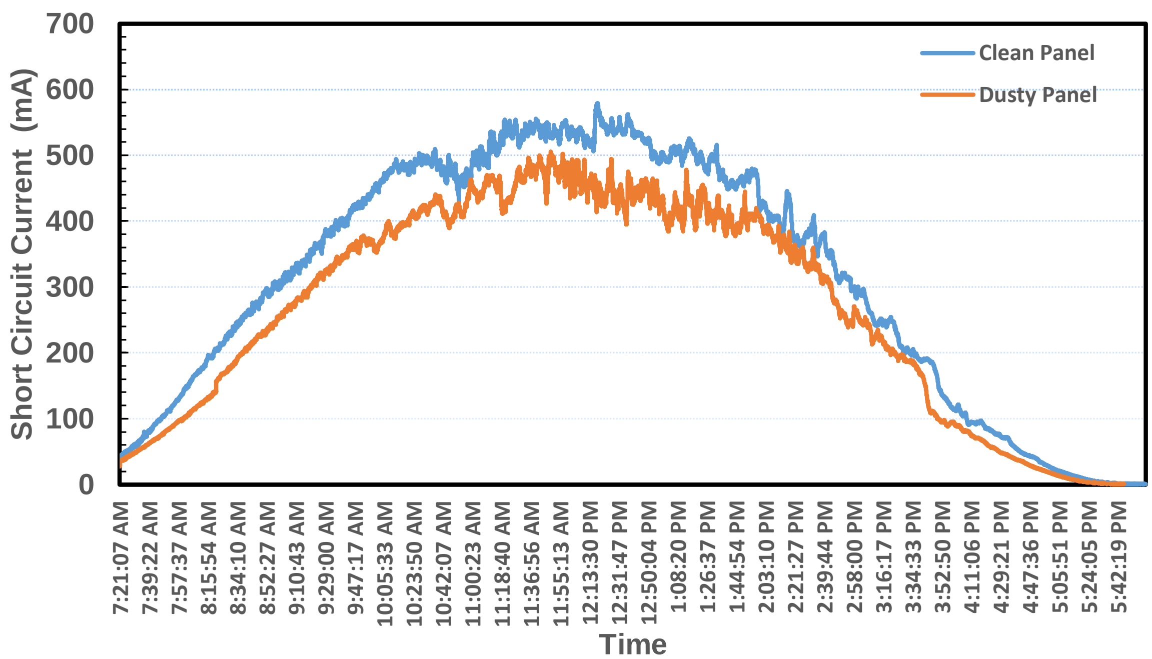

Figure 4.9: Plot of the Short Circuit Current of both clean and dusty solar panel collected on 12th January (Sunny Day)

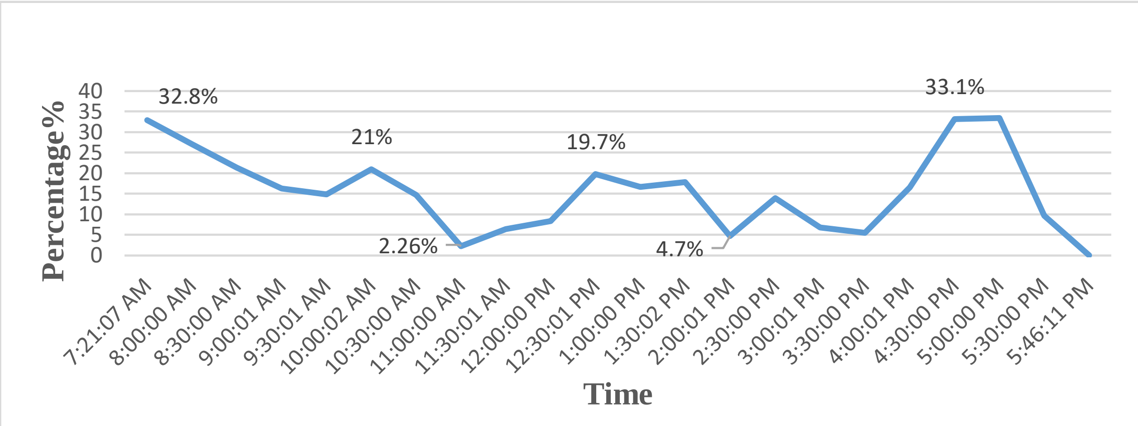

Figure 4.10: Plot of the Percentage difference of Short Circuit Current between clean and dusty solar panel collected on 12th January (Sunny Day)

Based on the data for January21, we can see from the graph in Figure 4.11, it was a cloudy day. Additionally, we can see that the output short circuit current for both the panel raises and drops several times w.r.t sunlight intensity, same as other cloudy days. However, the amounts vary significantly due to dust accumulation. On 21st January, the solar irradiance drops several times throughout the day, and so does the output short circuit current of both solar panels [23].and the percentage graph in Figure 4.12 doesn't shows much fluctuation either, except for once where the percentage reduction drop is 5.1%. Max output short circuit current of the clean and dusty solar panel was 593.3mA and 477.9mA respectively. The difference is quite noticeable and caused by dust accumulation.

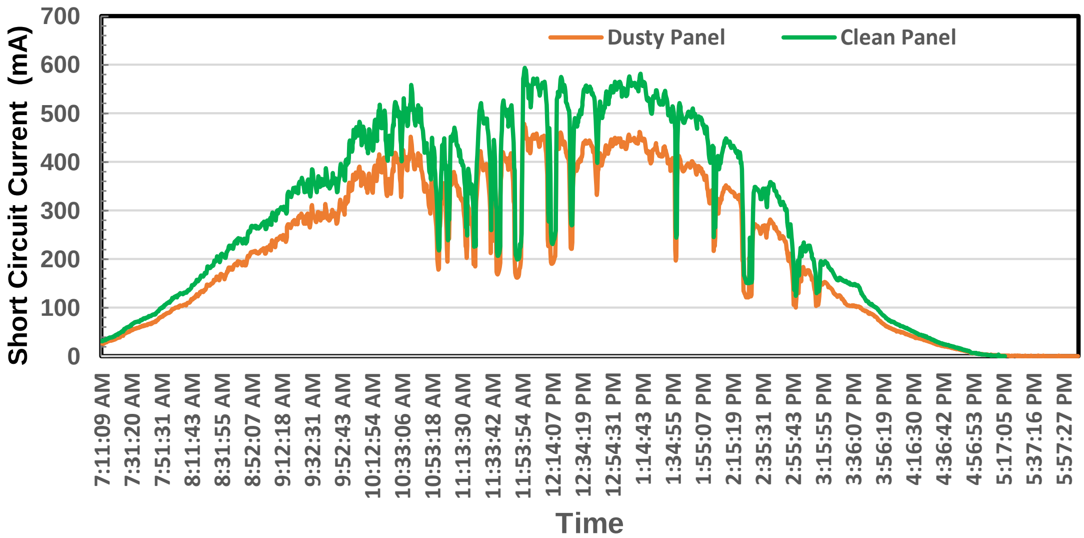

Figure 4.11: Plot of the Short Circuit Current of both clean and dusty solar panel collected on 21st January (Cloudy Day)

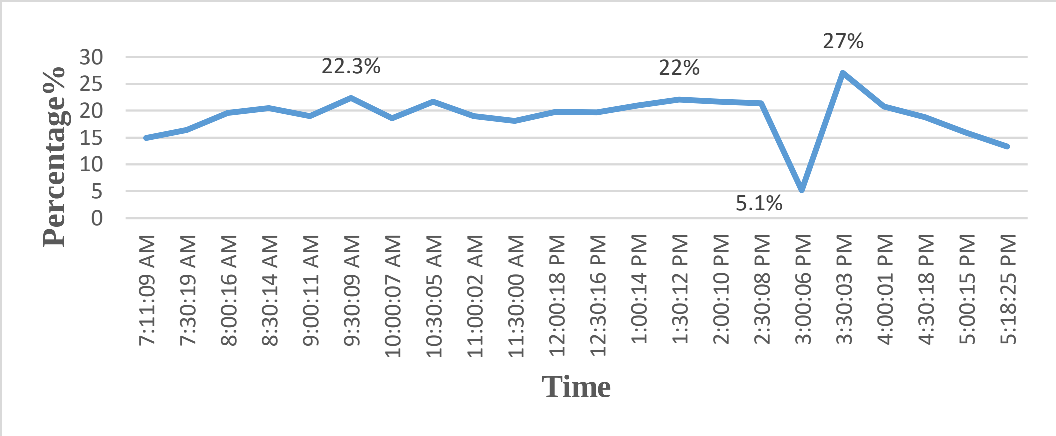

Figure 4.12: Plot of the percentage difference of Short Circuit Current between clean and dusty solar panel collected on 21st January (Cloudy Day)

Energy output:

Same output can be seen by the graph of the Energy Curve. Here we can see that on 5th December, In Fig 4.13, clean solar panel energy and dusty solar panel energy was slightly varied as it was only few days after the installation. which is **7.76%** lower than the clean module.

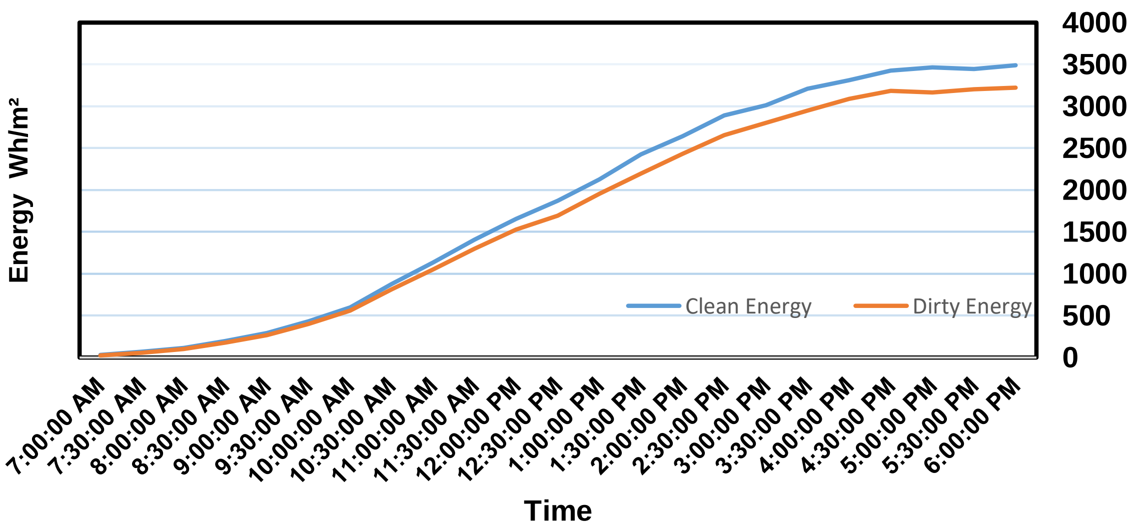

Figure 4.13: Plot of the cumulative Energy of both clean and dusty solar panel w.r.t time, recorded on 5th December

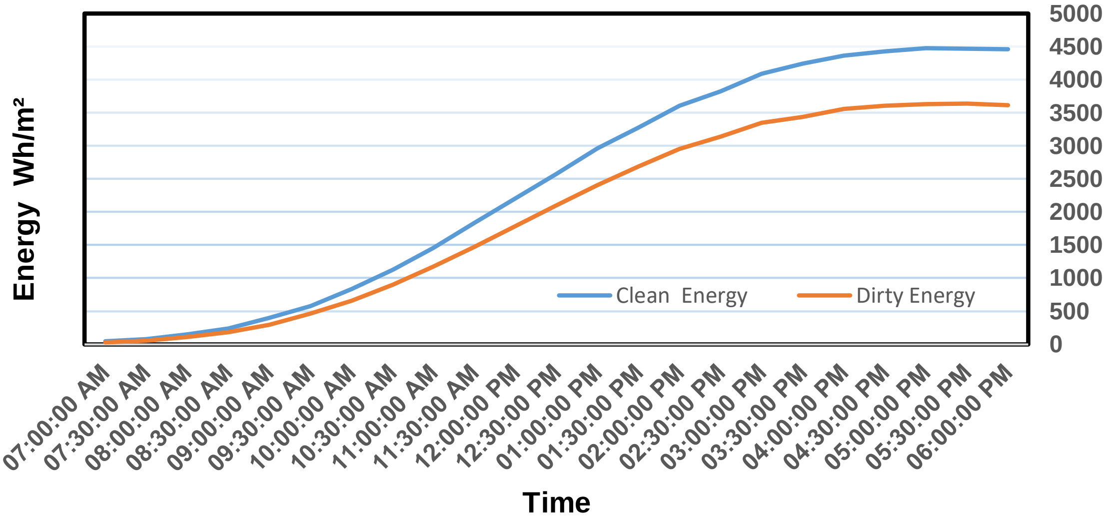

Figure 4.14: Plot of the cumulative Energy of both clean and dusty solar panel w.r.t time, recorded on 24th December

Looking at the energy curve of the 24th of December in Fig. 4.14, it can be seen that the clean solar panel energy output was quite high from the dusty solar panel. which is **18.94%** lower than the clean module So, the buildup dust particles do seem to have quite a toll on the solar output.

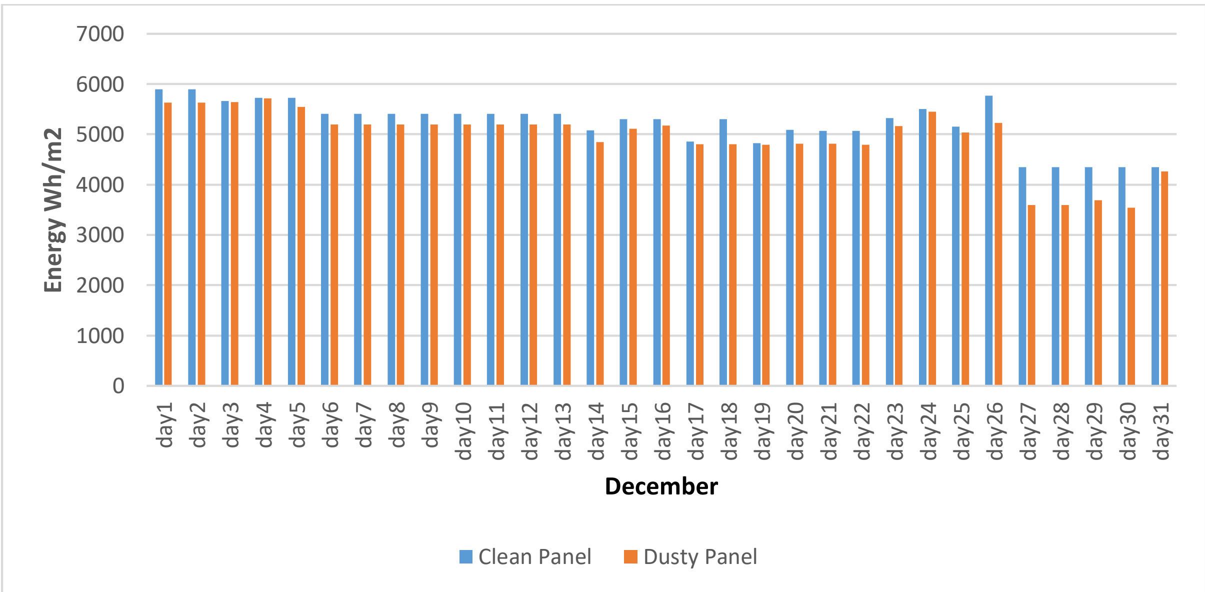

Figure 4.15: Plot of the total cumulative Energy of both clean and dusty solar panel w.r.t time, for the month of December

When examining the cumulative energy plot for both clean and dusty solar panel in Figure 4.15 for the month of December, a clear daily energy difference is observed. The energy output of the dusty panel is consistently lower compared the clean panel.

Similarly Figure 4.16 and Figure 4.17, which present the cumulative energy output for the month of January and February, respectively, display a similar trend, with the dusty panel generating less energy than clean panel.

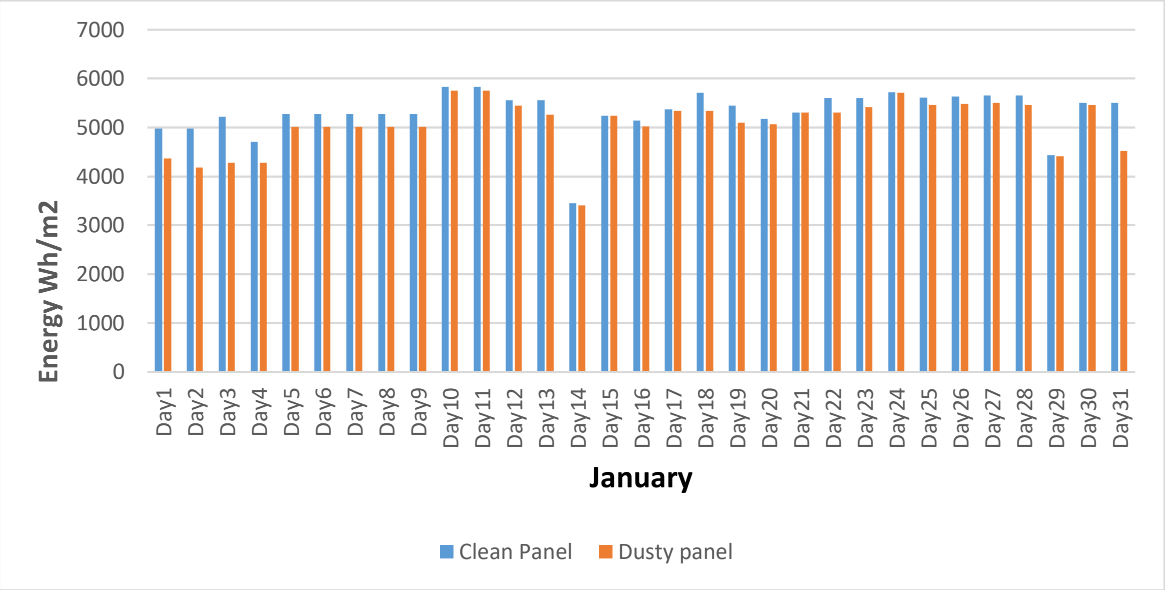

Figure 4.16: Plot of the total cumulative Energy of both clean and dusty solar panel w.r.t time, for the month of January

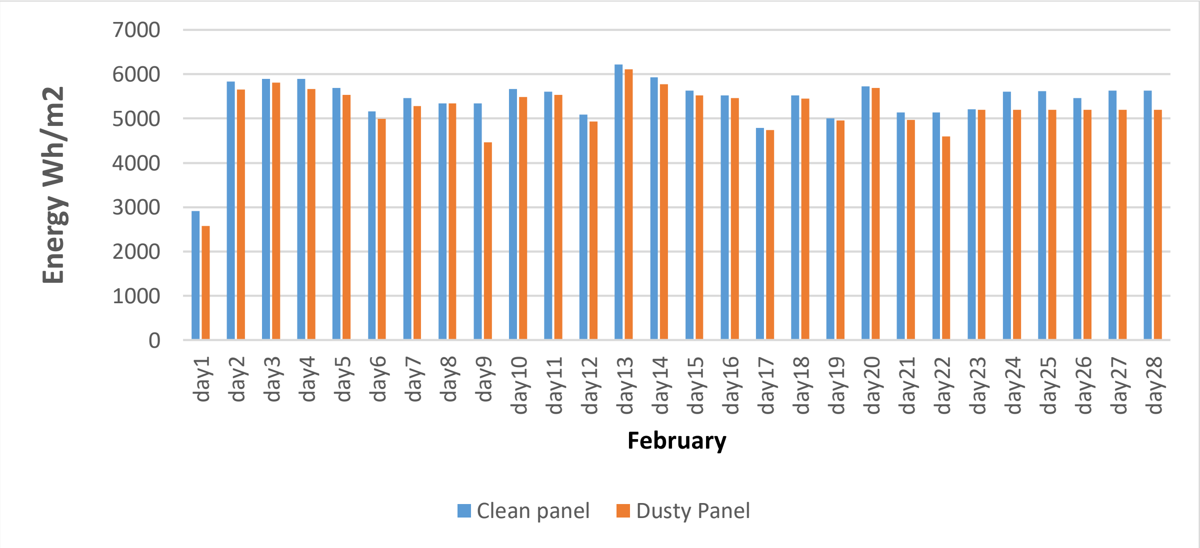

Figure 4.17: Plot of the total cumulative Energy of both clean and dusty solar panel w.r.t time, for the month of February.

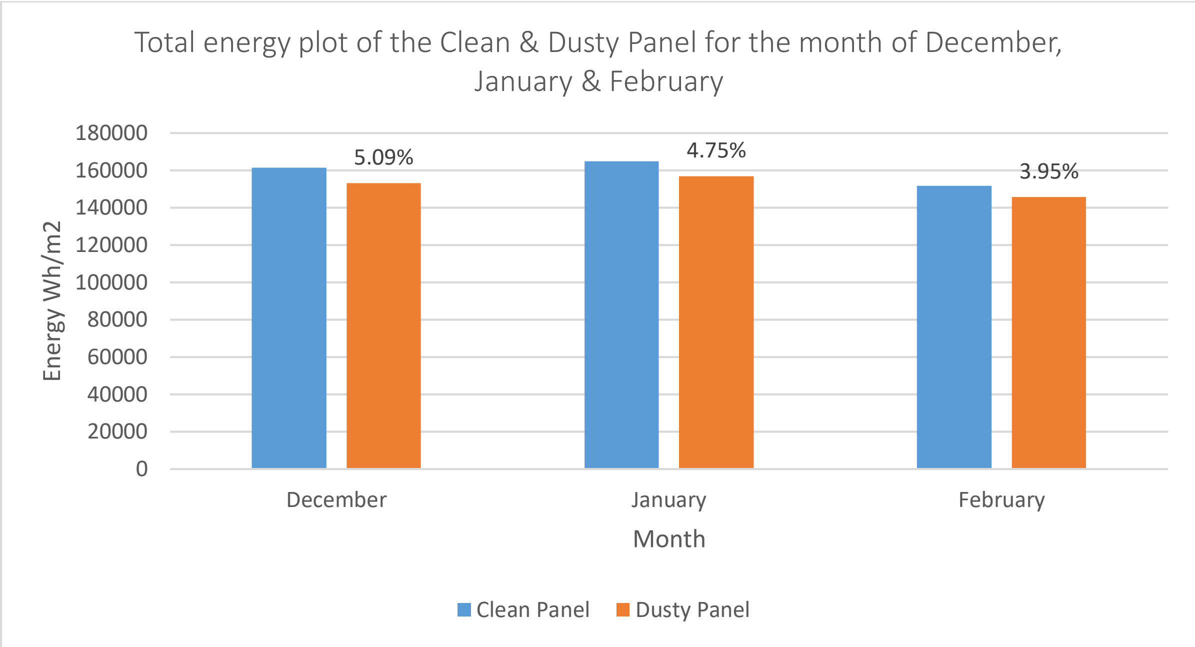

Figure 4.18: Plot of the total cumulative Energy of both clean and dusty solar panel for the month of December, January & February.

In the Figure 4.18 above, we can observe the difference in total energy output between the clean and dusty panel for the months of December, January & February. It is evident that the energy output from the clean solar panel is significantly higher than that of the dusty panel. Specifically, in December, the energy output of the dusty panel is **5.09%** lower than the clean panel. Similarly, the reduction in energy output for January and February, it is **4.75%** and **3.95%** respectively.

Weekly Variation:

A one-week plot is used to gain a better idea of how the dusty module's performance is degrading. Here we can see in Fig 4.19 we can see that the output short circuit current is decreasing. As dust particles accumulates, the output short circuit current decreases.

Figure 4.19 shows the trendline for the Short Circuit Current of the Dusty panel from 16th December to 22nd December. The trendline follows the equation for that week is:

$$y = -0.0105x + 361.69$$

this above equation represents a linear fit or trendline that describe the relation between time (or another independent variable x) and a short circuit current y generated by dusty panel. However, in a linear relationship, one variable (the dependent variable, y) changes in direct proportion to another variable (the independent variable x)[27].

The general equation for a linear relationship is [27] $y = mx + c$

Here, m is the slop line, representing the rate of change of y with respect to x. c is the y-intercept, represents the value of y when $x = 0$.

The slop in the following equation is -0.0105, this value represents the rate of change in the short circuit current with respect to independent variable (likely time or solar irradiance). Since the slop is negative, this indicates that independent variable x increases, such as time progress throughout the week, the short circuit current y slightly decreases. This suggest that over the week the dusty panel's performance degrade gradually, possible due to continuous dust accumulation.

The intercept is 361.69. this value represents the theoretical short circuit current when the independent variable x is zero. 361.69 is not a peak value, since it is simply where the trend line crosses the y-axis when x=0. This is the parameter of the trendline model and may differ from the mean or average value [27]. This intercept gives a baseline for how much current the panel generates at the start of the observation period and this value will depend on the condition of the dusty panel.

The negative slope, though small in magnitude, indicates a slight decline in the panel's performance as time progress.

This is a consistent with a fact that dust accumulation on solar panels typically leads to a gradual reduction in efficiency as the dust obstruct sunlight from reaching the solar cell [26].

The impact of the dust can be more pronounced over longer time periods, as shown by the gradual decline in the short circuit current.

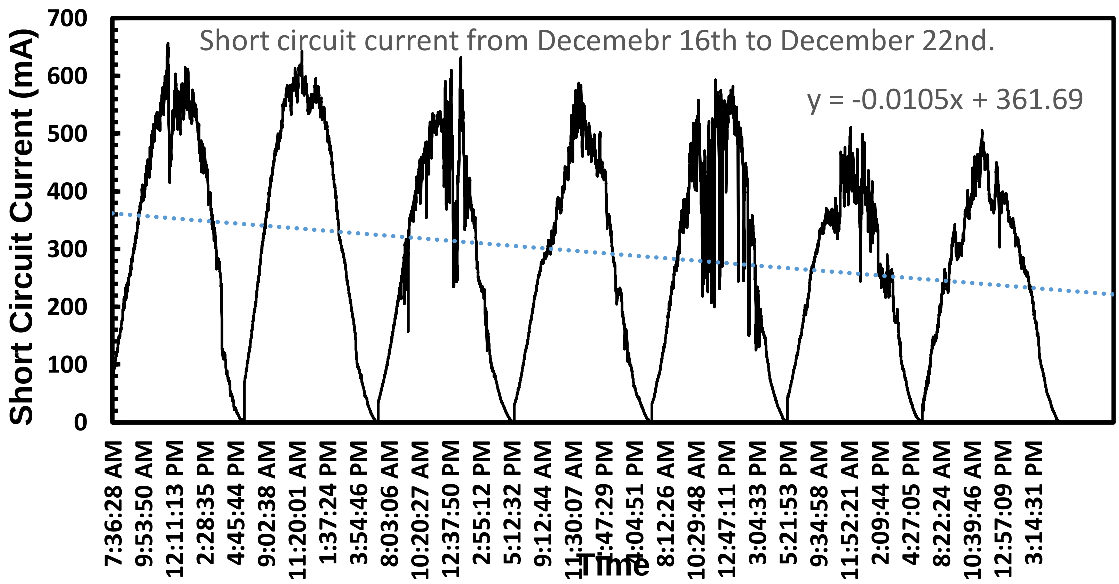

Figure 4.19: Trendline for the Short Circuit Current of the Dusty panel from 16th December to 22nd December

Similarly, one-week plot for the month of January & February is shown in Figure 4.20 & Figure 4.21. These plots provide a clearer understanding of how the dusty module's performance is degrading over time. It can be observed that as dust particles accumulates on the panel, the output short circuit current decreases.

Figure 4.20 presents the trend line for the Short Circuit Current of the Dusty panel from 19th January to January 25th. The trend line follows the equation for that week is:

y = -0.0051x + 224.84.

Additionally, Figure 4.21 shows the trend line for the Short Circuit Current from February 13th to February 19th, with the trend line following the equation:

y = -0.007x + 253.26 for that week.

Based on the above equation it can be concluded that, the dusty solar panel experience a slight decrease in short circuit current over the week. The negative slope represents the impact of ongoing dust accumulation, which reduces the amount of sunlight reaching the panel surface. As dust builds up, the panel's performance degrades, which is evident from gradual decrease of current output [25].

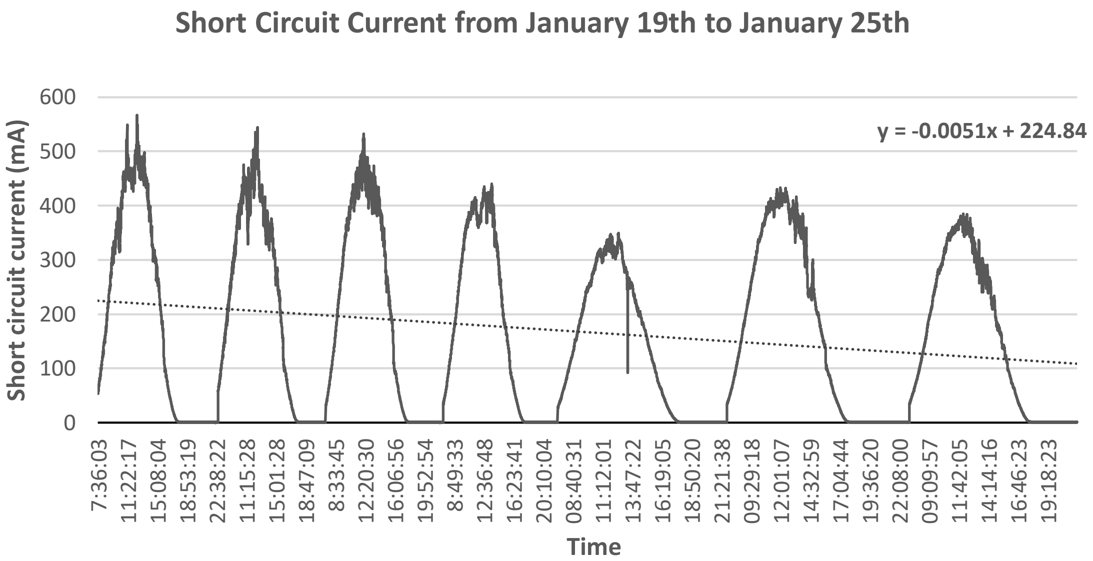

Figure 4.20: Trendline for the Short Circuit Current of the Dusty panel from 19th January to 25th January.

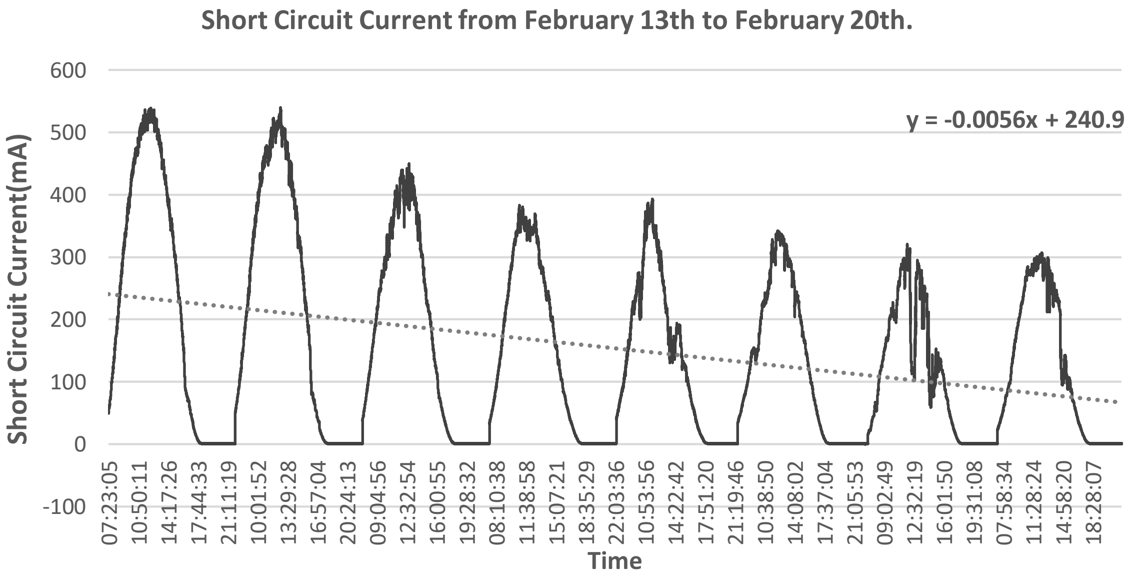

Figure 4.21: Trendline for the Short Circuit Current of the Dusty panel from 13th February to 19th February.

4.2 Predictive Analysis with Machine Learning

In this chapter, time series forecasting methods have been used for I_{sc} (mA) prediction for dusty module. Here, two distinct algorithms, **Facebook Prophet** and **LSTM** have been used as prediction models. Through our literature review, several algorithms have been identified which are capable of predicting short circuit current over a specified time period. However, analysis has been performed by deploying just two of such algorithms, further experimentation is possible. Here, current and temperature data were given as inputs to generate the I_{sc}values on specific days, particularly, 16th January and 23rd February. The input data included records for both one month and two-month periods. Furthermore, a comparison has been made on the predictive performance of these algorithms, using Root Mean Square Error (RMSE) values of the predicted results. This comparison is then used to conclude which algorithm performs better and how much effect solar intensity and dust has on the data over a period.

A technique known as time series forecasting is being used to predict the current output of a solar panel. The aim is to understand how the current changes over time, considering factors like temperature. To achieve this, the models were given one month and two months' data and the RMSE value for each simulation was observed. The whole process was done on google co-lab.

Initially, the necessary libraries, such as Facebook Prophet, are imported to aid in the development of the prediction models. The LSTM model is composed of an LSTM layer featuring 50 units, followed by a dense layer containing a single unit. The model is trained on the training data for 50 epochs with a batch size of 32.

Then, the data is loaded and prepared for analysis by creating timestamps and handling missing data. Any missing temperature values in the columns are filled with the last known value, thereby maintaining continuity in the data. Next, the data is divided into two parts: a training set and a testing set. In this case, 15% of the data was allocated to the testing set, while the remaining 85% was used for training. Furthermore, the data was split sequentially without shuffling, which is useful for time series data since the order of observations is important. The dependent and independent variables are also specified in this stage. The training set teaches the forecasting model about the relationship between current output over time. During training, the model learns patterns and connections in the data, which allows it to make predictions.

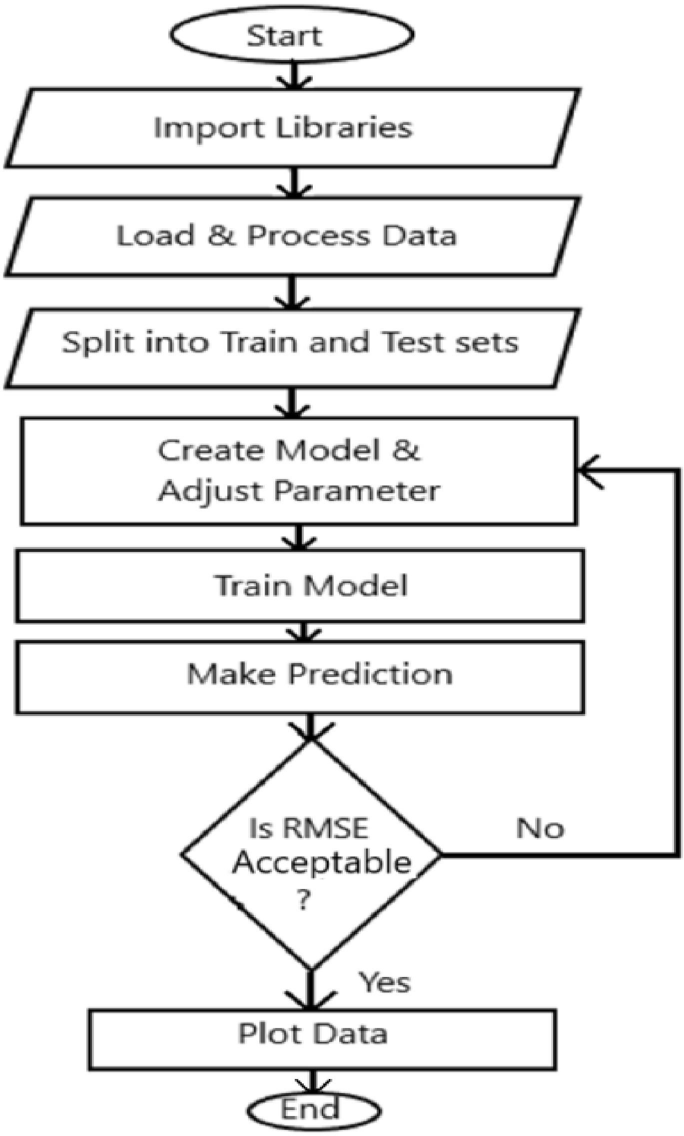

Figure 4.22: Flowchart of the working Procedure of the LSTM

Some parameters, like the strength of seasonality components and the mode of seasonality, are adjusted during this phase. Seasonal components were modeled as additive rather than multiplicative. This means that seasonal effects were added to the trend to produce the forecast. A higher value of the seasonality components indicates stronger correlation to the seasonality.

Once the model is trained, it is used to make predictions on the testing set. This set contains new data that the model hasn't seen before, enabling assessment of its performance on unseen data.

Future timestamps for prediction are adjusted, and any missing values in the future data are filled. Predictions are made using the trained model, and the results are visualized.

RMSE (Root Mean Square Error):

This is commonly used matric to measure the accuracy of a predictive model. It represents the square root of the average squared difference between actual value and the predicted values by the model [28]. The equation for RMSE is:

$$RMSE = \sqrt{\frac{1}{n}\sum_{i=1}^{n}(y_i - \hat{y_i})^2}$$

Where, y_i represent the actual value, $\hat{y_i}$ represent the predicted value and n, the number of data points.

In this study, the predicted values are compared with actual values from the testing set to evaluate the accuracy of the model. Here, we have used the RMSE metric here. The Root Mean Square Error or RMSE measures the differences between predicted values and actual values in the dataset by calculating the square root of the average of squared differences between predicted and observed values [28]. It indicates how well the forecasts generated by the two models align with the actual short circuit current values. A lower RMSE value signifies that the model's predictions are closer to the actual values, indicating higher accuracy. Thus, it serves as a quantitative measure of forecasting accuracy, guiding the selection and optimization of forecasting models. By repeating this process and fine-tuning parameters, the accuracy of predictions can be improved, providing insights into how temperature influences the current output of the solar panel over time. The process is shown in the Figure. 4.22.

4.2.1 FB Prophet Model

Prediction for 16th January using 1 month's data:

As we can see from the Figure 4.23, the actual and predicted values do not deviate much from each other except only at the start of the day. Here, prediction has been shown for only 1 day. The RMSE value for this plot was 69.56. This indicates that the predicted values differed from the actual values on average by 69.56 units [28], which is significantly high, considering that maximum value is itself around 600.

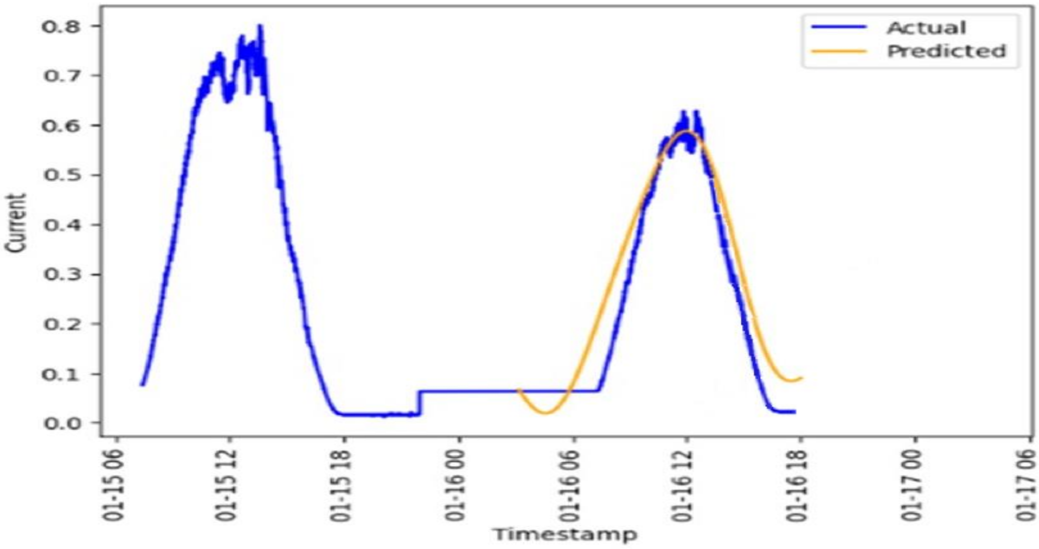

Figure 4.23: Predicted Plot of the dusty panel short circuit current, Data recorded on 16th January using FB Prophet Method. (FB prophet output Window)

Prediction for 23rd February using 1 month of data:

Here, in Figure 4.24 the actual and predicted values do not deviate much either. The RMSE value for this plot was 206.3. This indicates that the predicted values differed from the actual values on average by 206.3 units [28], which is significantly high. This can be since the day that was selected for prediction was further into the future than the first prediction. It can be assumed that the prediction accuracy decreases when the time interval is very large, in this case 1 month and 1 week into the future.

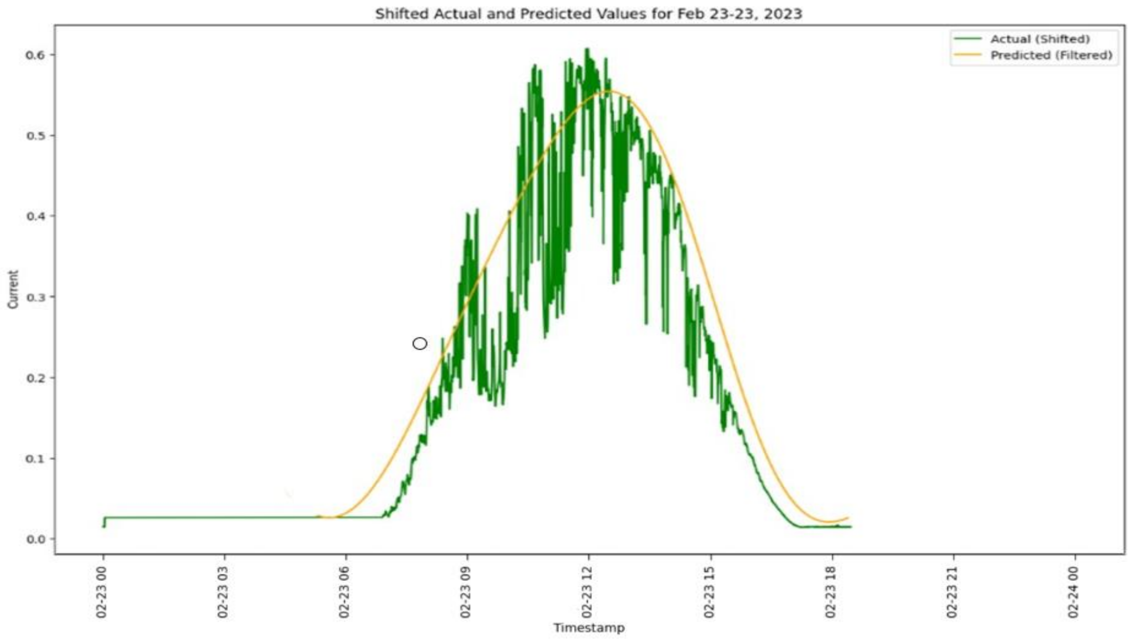

Figure 4.24: Predicted Plot of the dusty panel short circuit current, Data recorded on 23rd February using FB prophet Method (FB prophet output Window)

Prediction for 16th January using 2 months' data:

Here, in figure 4.25, the data set has been doubled. So, the model is now being trained on twice as much data. The RMSE value for this plot was **53.71**. This is lower than when the data set was half its size in the first case. This indicates that a larger dataset leads to better prediction, since the model now has more data to train on.

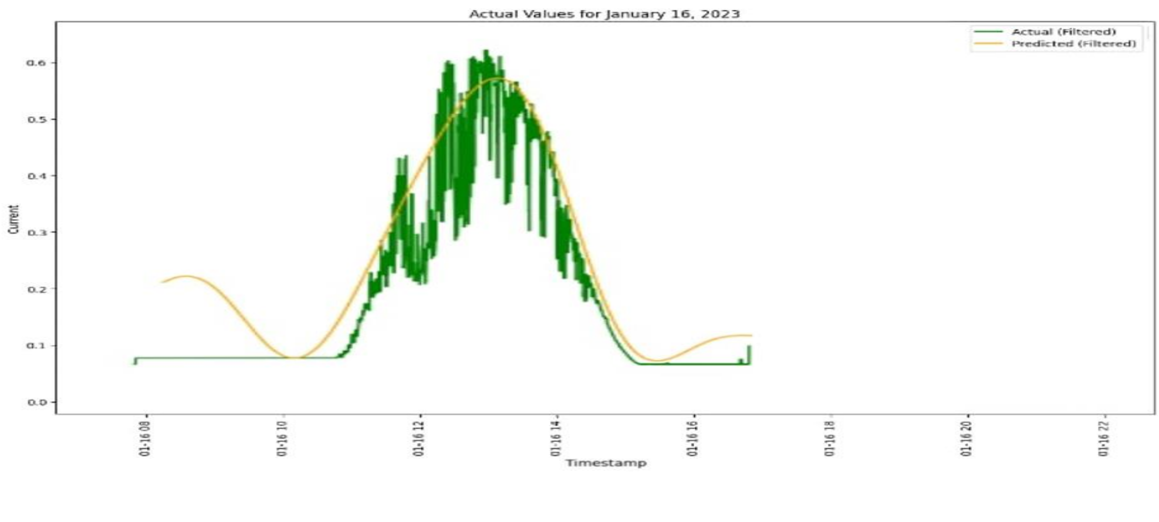

Figure 4.25: Predicted Plot of dusty panel short circuit current, Data recorded on 16th January using FB prophet method (FB prophet output Window)

Prediction for 23rd February using 2 months data:

This simulation was run using the dataset twice. Here, in Figure 4.26, the RMSE value for this plot was 130. This indicates that the predicted values differed from the actual values on average by 130 units [28]. In the previous case when the data set was half of its size, the RMSE value was around 200, so the accuracy improved. However, a value of 130 is still not acceptable, considering our average data value. Furthermore, it is important to note that even though the RMSE value has decreased, instantaneous fluctuations have not been accounted for in any of the simulations that were performed using this model.

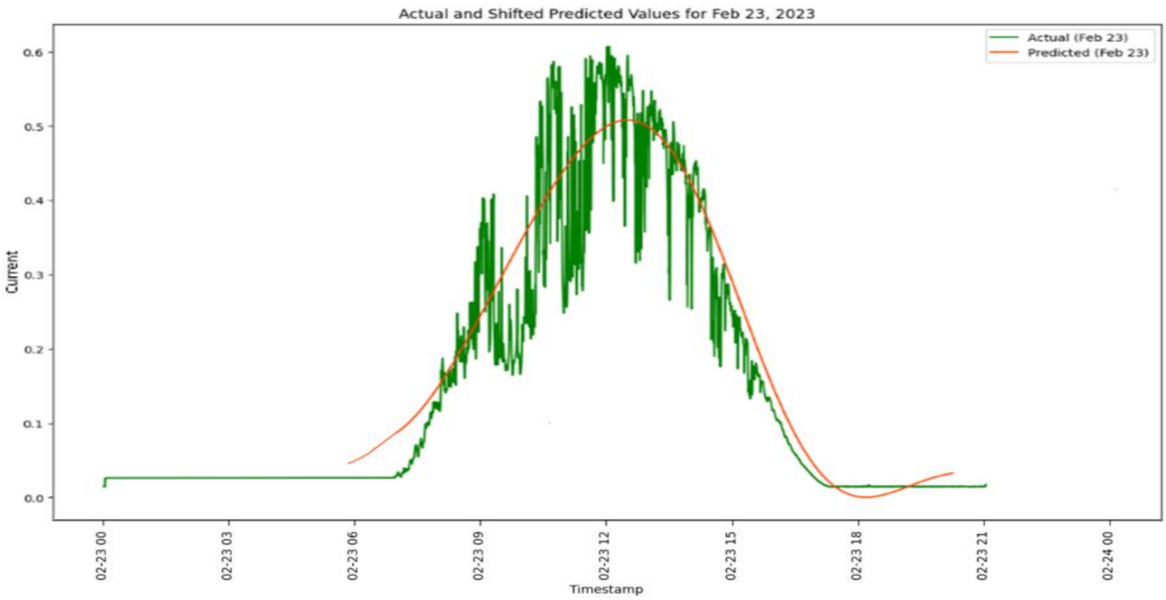

Figure 4.26: Predicted Plot of dusty panel short circuit current, Data recorded on 23rd February using FB prophet method (FB prophet output Window)

4.2.2 LSTM Model

16th January using 2 months data:

The prediction was done using LSTM as shown in Figure 4.27. The Figure 4.28 shows the output for 16th January particularly. 2 month's data was given as input and the RMSE value was 6.280 which was significantly lower than the previous prediction. This means that the actual and predicted values differed on average by 6 units which is negligible when the average current value is considered. This is significantly better than the prophet model. Also, the fluctuations in the daily graphs have been taken into consideration while predicting the values, which is also why the RMSE value is lower.

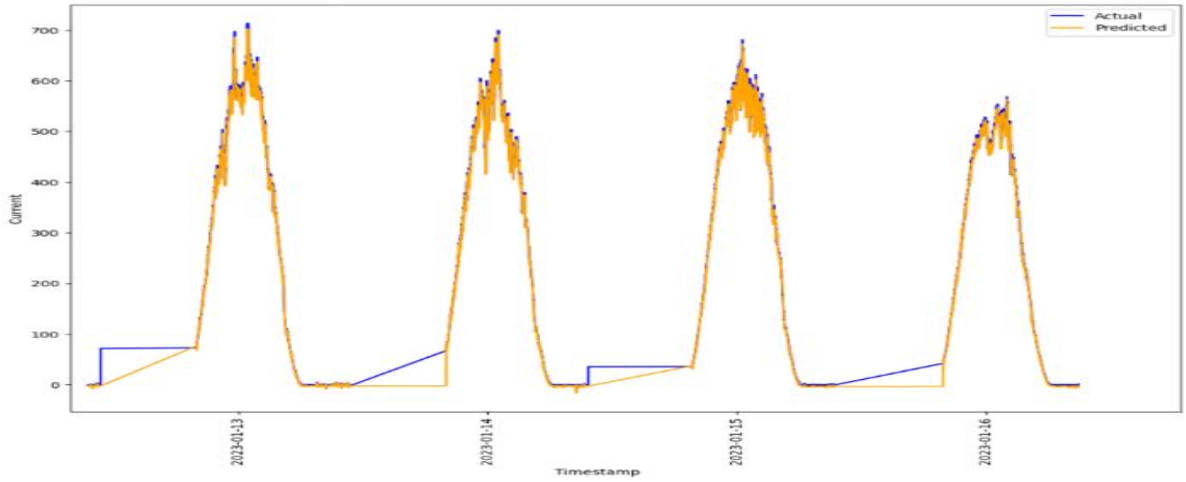

Figure 4.27: Predicted plot of dusty panel short circuit current, Data recorded on 13th to 16th January using LSTM method (LSTM output window)

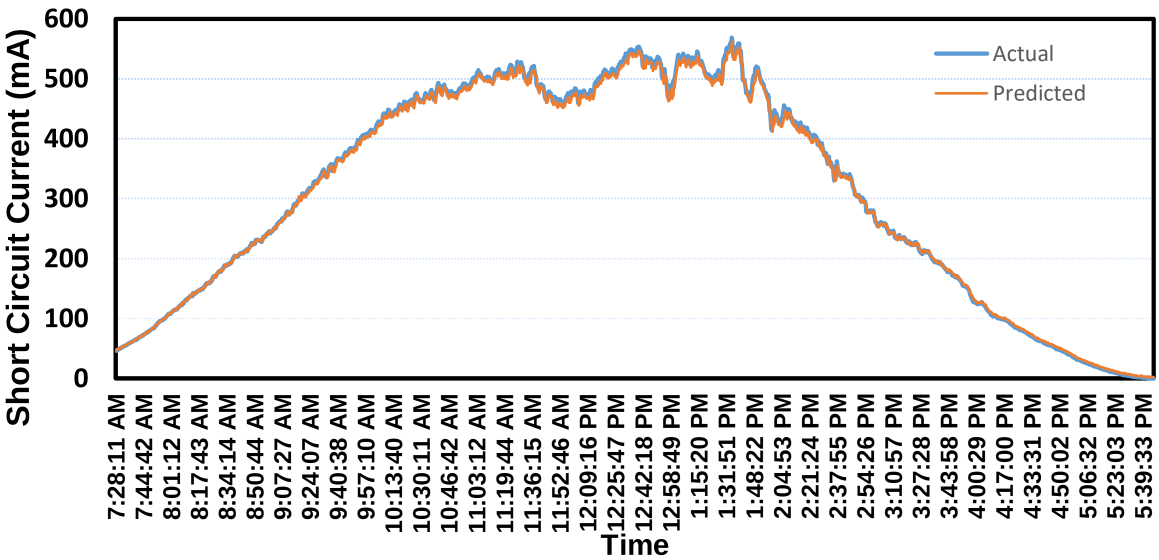

Figure 4.28: Predicted plot of dusty panel short circuit current, Data recorded on 16th January using LSTM method.

Prediction for 23rd February using 2 months data:

The prediction was done using LSTM as shown in Figure. 4.29. The Figure 4.30 shows the result output for 23rd January particularly. 2 months' data was given as input and the RMSE value was 11.46 which was significantly lower than the previous predictions using the Prophet model where the RMSE values were in the hundreds. This means that the actual and predicted values differed on average by 11 units [28] which is negligible when the average current value is considered. Also, the fluctuations in the daily graphs have been taken into consideration while predicting the values, which is also why the RMSE value is lower. Thus, we can conclude that the LSTM model is better at predicting the short circuit current than the Prophet model.

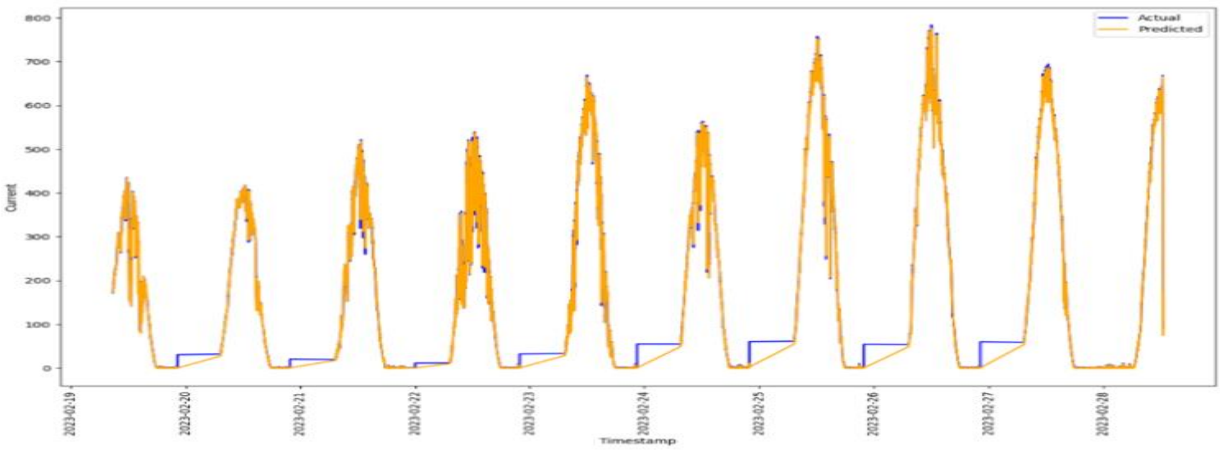

Figure 4.29: Predicted Plot of the dusty panel short circuit current, Data recorded from 19th to 28th February, using LSTM method.

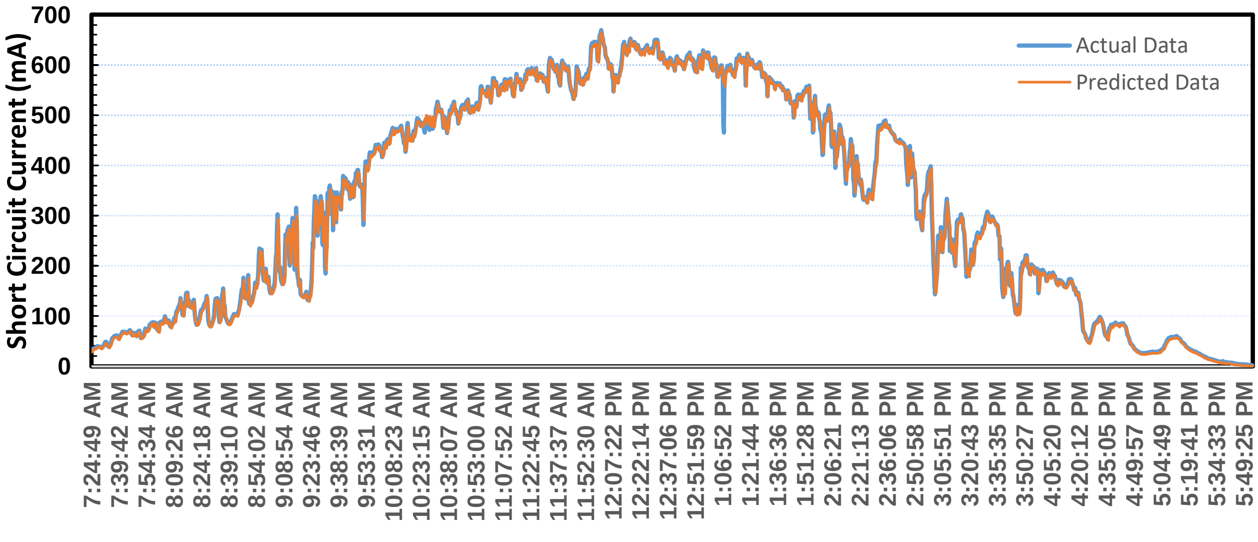

Figure 4.30: Predicted plot of the dusty panel short circuit current, Data recorded on 23rd February using LSTM method

4.3 Chapter Summary

The raw data analysis for both dusty and clean solar panels was covered in this chapter. Theoretical analysis is presented with in-depth information and an appropriate description of the factors related to the solar cell for both clean and dusty solar panels. Initially, the raw data analysis was displayed based on this study, which showed that the high solar intensity had a major influence on the solar panel's short circuit current.

Additionally, the effect of dust on solar panel performance is discussed, accompanied by an image of a dusty module and a comprehensive analysis of the daily variation in short circuit current for both clean and dusty modules. This analysis shows that the cumulative electrical output energy of the dusty module is lower than that of the clean module due to dust accumulation. The subsequent section presents the energy curve for both clean and dirty solar panels, along with a brief explanation; solar irradiance plays a crucial role in determining solar panel output, which is evident on both sunny and cloudy days. In summary, the theoretical analysis of both clean and dusty solar panels reveals that solar irradiance and dust particles significantly impact the output. Moving on to the predicted results, we can observe from the table below that."

After using two different models to predict the data of 16th January and 23rd February, it can be seen that LSTM performs very well compared to FB prophet. It was not possible to extract the data points from the FB prophet. That's why it was not possible to show the particular data points separately. But in case of the LSTM, these was easily extracted and was plotted for a better understanding of the predicted data compared to the real experimental data of those days. RMSE was 6.28 on 16th January and 11.46 on the 23rd of February. The prediction was far more accurate, and daily data changes were also taken into consideration. Nevertheless, the model's training period required a lot more time.

This thesis is based on data started collecting from December 2022 from two photovoltaic (PV) panels and environmental conditions such as Dust and Temperature. The extraction of data is accomplished by a synergistic combination of hardware and software, as detailed in Chapter 3. Table 5.1 shows the summarized result of this section.

Table 5.1: Comparison between output on 16th January and 23rd of February of FB prophet and LSTM

Model Used	Amount of input data	RMSE value on 16th January	RMSE value on 23rd February	Comments
FB Prophet	1 month	69.56	206.3	Model is not good at predicting data that is very far into the future.
	2 months	53.71	130	As more data was given for training, the prediction improved slightly. However, the model still could not follow the fluctuations of the actual data.
LSTM	2 months	6.280	11.46	Prediction was significantly better and fluctuations in the daily data were also accounted for. However, the time taken to train the model was significantly more.

Chapter 5

5.1 Conclusion

This thesis is based on data collected between December 2022 and February 2023 from two photovoltaic (PV) modules. This study focuses on analyzing the impact environmental conditions, particularly dust accumulation and solar irradiance on the performance of these panels. Data extraction was achieved through a combination of hardware and software, as described in Chapter 3. The research is divided into two primary sections: an analysis of the power output performance and a short-term prediction model for PV module efficiency.
This work primarily examines the performance of clean and dusty solar panels, considering environmental factors such as dust accumulation and solar irradiance. Both experimental and theoretical analysis are conducted, as detailed in Chapter 4. The short circuit current is directly proportional to solar irradiance, indicating that as sunlight intensity increases and temperatures rise, more energy can be generated. Additionally, dust plays a significant role in the performance of the solar module. In chapter 4, the impact of dust on solar panel performance is analyzed in various ways, leading to the conclusion that dust accumulation on the panel surface significantly degrades performance compared to a clean panel. While increased sunlight intensity causes a rise in the short circuit current of the PV module, this current is primarily influenced by solar irradiance, rather than other meteorological conditions.

Lastly, Chapter 4 also discusses short-term prediction analysis using FB prophet and LSTM models. This chapter demonstrates how lengthier training dataset, combined with two distinct RMSE comparisons, lead to more accurate and reliable predictions for the short circuit current of PV module on a given day. In the case of LSTM model, the predicted result closely matched the experimental data, with RMSE of 6.28 and 11.46 respectively. For future work, extending the dataset over a longer period would allow for a more comprehensive analysis of dust accumulation on both panels throughout the year.

5.2 Future Work

In the future work, long term data collection: extending the data collection period to cover multiple seasons or even years would allow for a more comprehensive analysis of the impact of various weather conditions, including dust accumulation over time. This could also provide the insight into seasonal variation in PV module performance.

Based on the data on dust accumulation, future research could focus on developing optimized cleaning schedules for PV panels to maximize efficiency and minimize maintenance costs. This could include both manual cleaning strategies and the potential automated or self-cleaning technologies.

Future work could include energy yield analysis over long term, evaluating the overall electricity generation under various environmental conditions and panel states (clean vs dusty)

Expanding the study to include different types of photovoltaic technologies such as, monocrystalline, polycrystalline, or thin film panels, which would help in understanding how environmental parameters affect different PV technologies.

Future work could explore the use of other advance machine learning techniques or hybrid model to improve better prediction accuracy, not only for short-circuit current but also overall energy output.

.

References

[1] O. Ellabban, H. Abu-Rub, F. Blaabjerg, “Renewable energy resources: Current status, future prospects and their enabling technology,” Renewable and Sustainable Energy Reviews, vol. 39, pp. 748-764, 2014.

[2] Bangladesh Power Development Board, [Online]. Available: https://www.bpdb.gov.bd/bpdb_new/index.php/site/page/5a3f-2fdb-e75f-3cab-e66b-f70d-5408-cbc9-f489-c31c [Accessed on August 2024]

[3] Hossain, M., Rabbi, F., Zaman, S., Rahman, F., & Islam, M. S. (2020). Study of Dust Effect on PV Panel’s Efficiency During Winter for Dhaka, Bangladesh. 2020 2nd International Conference on Sustainable Technologies for Industry 4.0 (STI).

[4] M. A. Kabir, R. Islam, S. Nazifa and R. Choudhury, "Dust Effect on Photovoltaic Output Performance: Comparative Analysis and A Case Study in Dhaka, Bangladesh," 2021 International Conference on Automation, Control and Mechatronics for Industry 4.0 (ACMI), Rajshahi, Bangladesh, 2021, pp. 1-6.

[5] T. Rahman et al., "Effects of Aging Factors on PV Modules Output Power: An Experimental Investigation," 2022 4th International Conference on Sustainable Technologies for Industry 4.0 (STI), Dhaka, Bangladesh, 2022, pp. 1-5.

[6] M. S. Alam, M. I. Islam and A. A. Mansur, "Comprehensive Investigation of Performance Degradation of Old Photovoltaic Panels at Outdoor Exposed Condition: A Case Study in Bangladesh," 2024 6th International Conference on Electrical Engineering and Information & Communication Technology (ICEEICT), Dhaka, Bangladesh, 2024, pp. 945-950.

[7] Md Shakil Ahmed, Raihan Karal, Barun K. Das, Arnob Das, “Experimental investigation of cooling, wind velocity, and dust deposition effects on solar PV performance in a tropical climate in Bangladesh,” Case Studies in Thermal Engineering,Vol. 50, 2023, no. 103409.

[8] P. G. Kale, K. K. Singh and C. Seth, "Modeling Effect of Dust Particles on Performance Parameters of the Solar PV Module," 2019 Fifth International Conference on Electrical Energy Systems (ICEES), Chennai, India, 2019, pp. 1-5.

[9] PV Education, [Online]. Available: https://www.pveducation.org/. [Accessed on August 2024]

[10] M. M. Rahman,.;M. Hasanuzzaman, N.A. Rahim, “Effects of various parameters on PV-module power and efficiency,” Energy Convers. Manag. Vol. 103, pp. 348–358, 2015.

[11] S.C.S. Costa, A.S.A.C. Diniz,; L.L. Kazmerski, Dust and soiling issues and impacts relating to solar energy systems: Literature review update for 2012–2015. Renew. Sustain. Energy Rev., vol. 63, pp. 33–61, 2016.

[12] Z.A.Darwish, H.A. Kazem, K. Sopian, M.A. Alghoul, M.T. Chaichan, Impact of Some Environmental Variables with Dust on Solar Photovoltaic (PV) Performance: Review and Research Status. Int. J. Energy Environ., vol.7,pp. 152–159, 2013.

[13] H. Abuzaid, M. Awad, & A. Shamayleh, ‘Impact of dust accumulation on photovoltaic panels: a review paper’. *International Journal of Sustainable Engineering*, vol. *15*(1), pp.264–285, 2022.

[14] M. Nezamisavojbolaghi, E. Davodian, A. Bouich, M. Tlemçani, O. Mesbahi, F. M. Janeiro, “The Impact of Dust Deposition on PV Panels’ Efficiency and Mitigation Solutions: Review Article.” *Energies*, vol. *16*, no. 8022, 2023.

[15] A. Shariah, E. Al-Ibrahim, ‘Impact of Dust and Shade on Solar Panel Efficiency and Development of a Simple Method for Measuring the Impact of Dust in any Location’, Journal of Sustainable Development of Energy, Water and Environment Systems, Vol. 11, no. 2, 2023.

[16] M.M.Rahman, M. Hasanuzzaman, N. A. Rahim, ‘Effects of various parameters on PV-module power and efficiency.’ Energy Convers. Manag. Vol.103, pp. 348–358, 2015.

[17] Taylor & Letham (2018), Forecasting at scale, FB Meta Prophet (Online) Available: https://facebook.github.io/prophet/docs/quick_start.html

[18] Geeksforgeeks.ord (Online) Available: https://www.geeksforgeeks.org

[19] lady ada, “Adafruit INA219 Current Sensor Breakout,” adafruit, October 26, 2012. [Online]. Available: https://learn.adafruit.com/adafruit-ina219-current-sensor-breakout.

[20] DALLAS SEMICONDUCTOR, “DS18B20 Programmable Resolution 1-Wire Digital Thermometer,” DALLAS SEMICONDUCTOR. [Online]. Available: https://image.dfrobot.com/image/data/DFR0198/DS18B20.pdf.

[21] Arduino and DS3231 Real Time Clock Tutorial – How To Mechatronics

[22] Component 101, "Arduino Uno," Component 101, February 28, 2018. [Online]. Available: https://components101.com/microcontrollers/arduino-uno.

[23] Tyagi,V.V, Rahim, N.A Rahim., N.A.,& Selvaraj.J.A.L(2013). Progresss in solar PV Technology: Research and Achievement, Renewable and Sustainable Energy Reviews,20,443-461.

[24] Luque. A., & Hegedus, S. (Eds). (2011). Handbook of Photovoltaic Science and Engineering. Green. M. A., Emery,K.,Hishikawa. Y., Warta, W.,& Zou, J.(2010). Solar efficiency tables (vol.34). Progress in Photovoltaics: Research and Applications,18(1)

[25] Qasem,H., Abdul-Majed, M., & Al-Shami, M.(2021). The impact of dust accumulation on the performance of photovoltaic panel in desert environment, Energy report, 7, 529-537.

[26] Mani. M., & Pillai, R. (2010). Impact of dust on solar photovoltaic (PV) performance: Research status, challenges, and recommendation, Renewable and Sustainable Energy Reviews,14(9), 3124-3131.

[27] Montgomery, D.C., & Runger, G.C (2010). Applied Statistics and Probability for Engineers. "Discussion of linear regression analysis and the method of least squares and fitting a line to data"

[28] Montgomery. D.C., Peck, E.A., & Vining, G.G (2012). Introduction to Linear Regression analysis, James, G., Witten, D., Hastile, T,. & Tibshirani, R. (2013). An Introduction to statistical Learning with Application in R.

[29] Baojie Li, Anne Migan-Dubois, Claude Delpha, Demba Diallo. Irradiance Dependence of the Short-Circuit Current Temperature Coefficient of sc-Si PV Module. IEEE Photovoltaic Specialists Conference (PVSC 2020), Jun 2020, Calgari (virtual), Canada. ff10.1109/PVSC45281.2020.9300416 hal-02903351

[30] Hyndman & Athanasopoulos (2018), Forecasting: Principle & Practice " A foundation of time series forecasting method", Brownlee (2017), Deep learning for Time series Forecasting.

Appendix A

Solar Module Specification

Module Type	Poly-10W
Maximum Power (P_{max})	10W
Tolerance of P_{max}	0±3%
Rated Voltage (V_{mp})	17.5V
Rated Current (I_{mp})	0.61A
Open-Circuit Voltage (V_{oc})	21.6V
Short-Circuit Current (I_{sc})	0.56A
Maximum System Voltage	1000V
Operating Temperature	-40°C to +85°C
Weight	2.3Kg
Dimension(mm)	355*290*17
Manufactured	Japan

Technical performance data recorded at Standard Test Conditions (STC) Am = 1.5, E=1000W/m2, TC= 25°C

Appendix B

LSTM Code

```
import pandas as pd
import numpy as np
import matplotlib.pyplot as plt
from sklearn.preprocessing import MinMaxScaler
from sklearn.model_selection import train_test_split
from tensorflow.keras.models import Sequential
from tensorflow.keras.layers import LSTM, Dense

# Load and preprocess data
glass = pd.read_csv('/content/y.csv')
glass['Timestamp'] = pd.to_datetime(glass['Date'] + ' ' + glass['Time'])
glass.set_index('Timestamp', inplace=True)

# Check for and remove duplicate timestamps
glass = glass[~glass.index.duplicated(keep='first')]

# Fill NaN values in the 'Temp' column with the mean
glass['Temp'].fillna(method='ffill', inplace=True)

# Select relevant columns
glass = glass[['Current', 'Temp']]

# Separate scalers for 'Current' and 'Temp' columns
scaler_current = MinMaxScaler()
scaler_temp = MinMaxScaler()

glass[['Current']] = scaler_current.fit_transform(glass[['Current']])
glass[['Temp']] = scaler_temp.fit_transform(glass[['Temp']])
```

```python
# Train-Test Split
train_data, test_data = train_test_split(glass, test_size=0.15, shuffle=False)

# Prepare data for LSTM
def create_dataset(X, y, time_steps=1):
    Xs, ys = [], []
    for i in range(len(X) - time_steps):
        Xs.append(X.iloc[i:(i + time_steps)].values)
        ys.append(y.iloc[i + time_steps])
    return np.array(Xs), np.array(ys)

time_steps = 10
X_train, y_train = create_dataset(train_data[['Current', 'Temp']], train_data['Current'], time_steps)
X_test, y_test = create_dataset(test_data[['Current', 'Temp']], test_data['Current'], time_steps)

# Build LSTM model
model = Sequential()
model.add(LSTM(units=50, input_shape=(X_train.shape[1], X_train.shape[2])))
model.add(Dense(units=1))
model.compile(optimizer='adam', loss='mean_squared_error')

# Train the model
model.fit(X_train, y_train, epochs=50, batch_size=32, verbose=1)

# Make predictions
y_pred = model.predict(X_test)
```

```python
# Make predictions
y_pred = model.predict(X_test)

# Inverse transform the predicted values to the original scale
y_pred_original_scale = scaler_current.inverse_transform(y_pred)
y_test_original_scale = scaler_current.inverse_transform(y_test.reshape(-1, 1))

# Plot the actual and predicted values for the last two days
fig, ax = plt.subplots(figsize=(15, 9))
plt.plot(test_data.index[time_steps:], y_test_original_scale, label='Actual', color='#0000FF')
plt.plot(test_data.index[time_steps:], y_pred_original_scale, label='Predicted', color='#FFA500')
plt.xlabel('Timestamp')
plt.xticks(rotation=90)
plt.ylabel('Current')
plt.legend()
plt.show()
```

/////////

FB Prophet Code

```
import pandas as pd
import numpy as np
import matplotlib.pyplot as plt
from sklearn.model_selection import train_test_split
from prophet import Prophet
from sklearn.preprocessing import MinMaxScaler
# Load and preprocess data
glass = pd.read_csv('/content/f.csv')
glass['Timestamp'] = pd.to_datetime(glass['Date'] + ' ' + glass['Time'])
glass.set_index('Timestamp', inplace=True)

# Check for and remove duplicate timestamps
glass = glass[~glass.index.duplicated(keep='first')]

# Fill NaN values in the 'Temp' column with the mean
glass['Temp'].fillna(method='ffill', inplace=True)

# Select relevant columns
glass = glass[['Current', 'Temp']]

# Separate scalers for 'Current' and 'Temp' columns
scaler_current = MinMaxScaler()
scaler_temp = MinMaxScaler()

glass[['Current']] = scaler_current.fit_transform(glass[['Current']])
glass[['Temp']] = scaler_temp.fit_transform(glass[['Temp']])

# Train-Test Split
train_data, test_data = train_test_split(glass, test_size=0.15, shuffle=False)
```

```python
train_data.reset_index(inplace=True)
prophet_data = train_data.rename(columns={'Timestamp': 'ds', 'Current': 'y', 'Temp': 'temp'})

# Initialize and fit the Prophet model
model = Prophet(seasonality_mode='additive', seasonality_prior_scale=17)
model.add_regressor('temp')
model.fit(prophet_data)

# Generate future timestamps for forecasting
future = model.make_future_dataframe(periods=len(test_data), freq='40S')

# Fill NaN values in the 'Temp' column of the future dataframe with the mean
future['temp'] = scaler_temp.transform(np.full((len(future), 1), glass['Temp'].mean())).flatten()

# Make predictions
forecast = model.predict(future)

forecast['yhat_original_scale'] = scaler_current.inverse_transform(forecast[['yhat']].values)

# Extract actual values for the last two days
last_two_days_actual = glass.loc[glass.index.date >= glass.index.max().date() - pd.DateOffset(days=1)]

# Filter forecast data for the last two days
last_two_days_forecast = forecast[forecast['ds'].dt.date >= forecast['ds'].max().date() - pd.DateOffset(days=1)]
```

```python
# Plot the actual and predicted values for the last two days
fig, ax = plt.subplots(figsize=(15, 9))
plt.plot(last_two_days_actual.index, last_two_days_actual['Current'], label='Actual', color='#0000FF')
plt.plot(last_two_days_forecast['ds'], last_two_days_forecast['yhat'], label='Predicted', color='#FFA500')
plt.xlabel('Timestamp')
plt.xticks(rotation=90)
plt.ylabel('Current')
plt.legend()
plt.show()
```